INFORMATION TO USERS

This manuscript has been reproduced from the microfilm master. UMI films the text directly from the original or copy submitted. Thus, some thesis and dissertation copies are in typewriter face, while others may be from any type of computer printer.

The quality of this reproduction is dependent upon the quality of the copy submitted. Broken or indistinct print, colored or poor quality illustrations and photographs, print bleedthrough, substandard margins, and improper alignment can adversely affect reproduction.

In the unlikely event that the author did not send UMI a complete manuscript and there are missing pages, these will be noted. Also, if unauthorized copyright material had to be removed, a note will indicate the deletion.

Oversize materials (e.g., maps, drawings, charts) are reproduced by sectioning the original, beginning at the upper left-hand corner and continuing from left to right in equal sections with small overlaps.

ProQuest Information and Learning
300 North Zeeb Road, Ann Arbor, MI 48106-1346 USA
800-521-0600

Differential and Coherent RAKE Receivers for DS-CDMA in Frequency-Selective Rayleigh Fading Channels

by
Claude D'Amours, B.A.Sc.

A thesis submitted to the
School of Graduate Studies and Research
in partial fulfillment of the requirements
for the degree of
Master of Applied Science

Ottawa-Carleton Institute for Electrical Engineering
Faculty of Engineering
Department of Electrical Engineering
University of Ottawa

Differential and Coherent RAKE Receivers for DS-CDMA in Frequency-Selective Rayleigh Fading Channels

by
Claude D'Amours, B.A.Sc.

Abstract

The performance of digital communications over frequency-selective Rayleigh fading channels can be quite poor, thus diminishing the capacity of a DS-CDMA system. This thesis compares differential detection, multiple symbol differential detection and pilot symbol-aided coherent detection of a direct-sequence spread spectrum signal for this channel. Diversity reception is obtained through RAKE reception, and both equal gain and maximal gain diversity combining are considered. The improvement provided by some error correcting convolutional codes and interleaving are also studied.

Acknowledgements

This research was made possible due to the efforts of many individuals. At this point, I would like to express my gratitude to these individuals.

I would like to thank the Communications Research Centre, especially Michael Moher, for providing the software, LINKSIM, funding and an outline for this research.

I would also like to express my gratitude to my supervisor, Dr. Abbas Yongaçoğlu, who acted as team manager for the duration of this research. His knowledge and hard work was instrumental in the completion of this work.

I would also like to thank Richard Young of the Communications Research Centre for taking the time to familiarize me with the software package, LINKSIM.

Jun Wang of the University of Ottawa was also instrumental in the completion of this research. He translated the software from IBM to UNIX which greatly increased the speed of the simulations.

Finally, I would like to thank my family for their support throughout my studies at the University of Ottawa.

Contents

List of Figures

List of Tables

List of Abbreviations

AWGN - additive white Gaussian noise.

BER - bit error rate.

BPSK - binary phase shift keying.

CDMA - code division multiple access.

CRC - Communications Research Centre.

CW - continuous wave.

DBPSK - differential binary phase shift keying.

DC - direct current.

DD - differential detection.

DPSK - differential phase shift keying.

DS - direct sequence.

DS-CDMA - direct sequence code division multiple access.

FCC - Federal Communications Commission.

FSK - frequency shift keying.

ISM - Industrial, Scientific and Medical.

MSDD - multiple symbol differential detection.

PCN - personal communications network.

PN - pseudonoise.

PSA - pilot symbol-aided detection.

PSK - phase shift keying.

r1/2c7 - rate 1/2 constraint length 7 convolutional code.

r1/4c7 - rate 1/4 constraint length 7 convolutional code.

r1/8c7 - rate 1/8 constraint length 7 convolutional code.

SAW - surface acoustic wave.

TCM - trellis coded modulation.

List of Symbols

$a_i(t)$ - complex, time-varying coefficient of ith path in multipath channel.

B_c - spreading factor.

B_d - Doppler spread of multipath channel.

C - total power of signal.

E_b - received energy per bit.

$(E_b/N_o)_{eq}$ - equivalent energy per bit to spectral noise density ratio of diversity combining system.

E_c - received energy per chip.

E_{cs} - received energy per code symbol.

f_{ns} - carrier frequency of non-spread interference signal.

f_{ss} - carrier frequency of spread spectrum signal.

I - power in interference signal.

K - number of chips in one period of PN sequence.

K_a - number of chips in one period of augmented PN sequence.

K_m - number of chips in one period of maximal-length PN sequence.

M - number of simultaneous users in a CDMA system.

M_{max} - maximum number of simultaneous users in a CDMA system.

N_o - single-sided noise power spectral density.

N_o' - equivalent single-sided noise power spectral density of CDMA system.

$P_{av}(L)$ - average effective power of Lth order diversity system.

p_b - probability of bit error.

$p_b(L)$ - probability of bit error of Lth order diversity system.

r - code rate.

R_b - bit rate.

R_c - chip rate.

R_{cs} - code symbol rate.

T_b - bit duration.

T_c - chip duration.

T_m - multipath spread of channel.

T_{td} - transmission delay.

$T_i(t)$ - time-varying delay of ith path in multipath channel.

V - voice activity factor.

w_i - weighting factor of ith path for maximal gain diversity.

W_{ns} - bandwidth of non-spread interference signal.

W_{ss} - bandwidth of spread spectrum signal.

$(\Delta f)_c$ - coherence bandwidth of multipath channel.

η - spectral efficiency.

γ' - minimum energy per bit to spectral noise density required for acceptable BER.

$\bar{\gamma}_c$ - average energy per bit to spectral noise density per diversity path.

$\theta_i(t)$ - time-varying phase of ith path in multipath channel.

Chapter 1

Introduction

The telecommunications industry is currently undergoing a technological revolution which is fuelled by the demand for wireless communications services. These services include cordless telephones, pagers and cellular telephones. Presently, there are more than 4.5 million cellular phones in use in the United States [1], and the need for this service is growing rapidly. Many believe that the existing allocated cellular bandwidths are insufficient to support the number of users that the service will draw. In fact, cellular operators are reaching their maximum capacity in several cities today [2].

Personal Communications Networks (PCNs) are now being aggressively proposed as the logical evolution of cellular telephone. The technology would allow the use of a small portable communication device from virtually anywhere in the world by combining wireless, satellite, and wireline communications. PCN's strongest supporters believe that eventually 25 to 60 million consumers in the United States would subscribe to this service [2]. Currently, the bandwidth required to support such a huge number of users is unavailable as much of the allocated frequency spectrum is already occupied.

New method of spectrum utilization are now being investigated in order to improve spectrum efficiency. Currently in North America, there are four major companies that are investigating the use of code division multiple access (CDMA), which op-

erates using spread spectrum technology, as a means to increase capacity in the current cellular telephone networks and as a possible strategy in the implementation of PCNs. These companies are Cylink, Omnipoint Data, Millicom, and Qualcomm [2]. They believe that spread spectrum can offer many benefits in the implementation of future wireless services. The three primary advantages are:

i) Because of the congested nature of the frequency spectrum in the United States, it is unlikely that the large bandwidths needed for these future services will be available. The sharing of radio spectrum with existing communication users, especially point-to-point microwave towers (1700-2300 MHz) [2,3] is made possible through spread spectrum. The anti-jam and low density properties of spread spectrum signals would allow the co-existance of spread spectrum with existing users.

ii) Spread spectrum is the only technology that allows for the full exploitation of the voice activity factor which in turn increases the number of users in cellular networks [4,5,6]. The voice activity factor is about 35%. When users assigned to the channel are not transmitting, the mutual interference is reduced. Thus, the voice activity factor reduces the mutual interference by about 65%, increasing the true channel capacity by a factor between 2 and 3.

iii) New FCC and Canadian DOC regulations allow the unlicensed use of spread spectrum on certain RF bands, notably the Industrial, Scientific, and Medical (ISM) equipment bands at 902-928, 2400-2483.5 and 5725-5850 MHz [7]. These frequencies are used for non-communication purposes, and thus the FCC allows spread spectrum users to transmit up to 1 W of power in these bands.

A direct sequence CDMA signal consists of a transmitted signal which is spread over the entire bandwidth of the communications system by a pseudo-noise (PN) sequence. All other users occupy this bandwidth as well. At the receiver, the desired signal is recovered by despreading the signal with the proper PN sequence. All undesired signals remain spread over the entire bandwidth. If the number of simultaneous users is large, using the central limit theorem, the multiuser interference can be approximated as equivalent to additive white Gaussian noise [8]. In the general case, if PN sequences with good correlation properties are used (eg. m-sequences, Gold sequences), the AWGN equivalence is a conservative approximation [9]. Therefore, as additional users transmit over the channel, the

performance of each user degrades. Because of this, the system is power limited. The capacity is determined by how many simultaneous users the system can sustain while maintaining an acceptable level of performance. Thus, optimization of the performance of a CDMA system is needed in order to optimize its capacity.

One of the greatest impairments to mobile radio is the multipath-induced fading nature of the channel. An inherent advantage of using CDMA is its amelioration of the effects of multipath. As the receiver despreads one path, all other echoes appear as nearly equivalent to white noise, thus reducing its ability to degrade the system performance. The ability of direct-sequence (DS) spread spectrum to resolve individual paths from the overall multipath signals allows for the reception of many paths if RAKE reception is used. This results in the improved performance through diversity combining, which in turn increases system capacity. The diversity combining method is important in the optimization of the system's performance.

The choice of detection technique is also an important factor in the optimization of the system's performance. In a frequency-nonselective Rayleigh fading channel, coherent detection provides a 3dB advantage over differential detection and a 6dB gain over orthogonal signalling [10]. This advantage is maintained when the channel is frequency-selective and the available diversity is exploited. Such large gains can greatly increase capacities in CDMA systems. However, coherent detection requires some form of channel phase estimation. The performance of such a system will depend greatly on the reliability of the channel phase estimates. Channel sounding is generally used in channel phase estimation [11]. An alternative technique which is well suited for this type of channel is differential detection because it does not require a carrier phase recovery circuit. Recent results in literature indicate that the performance of differential detection in an additive white Gaussian noise channel can approach that of coherent detection by observing the phase change over a number of symbols [12,13]. This is known as multiple symbol differential detection (MSDD). Since improved performance translates into higher capacities, an optimum detection scheme must be determined for the land mobile channel.

In addition to the diversity advantage of direct-sequence spread spectrum systems with RAKE receivers, coding is another way by which time diversity can be intro-

duced and the performance in a frequency selective Rayleigh fading channel can be further improved. Along with the diversity gain obtained from the channel and the nature of the spread spectrum signal, a good detection/coding scheme can be found which would greatly increase the capacity of the CDMA channel.

1.1 Multipath Channel Model

A brief description of the frequency-selective Rayleigh fading channel model is discussed in this section as it forms the foundation of all research discussed in this thesis.

The land mobile channel is a hostile environment for signal propagation. Terrain, buildings, and other mobiles are some of the obstacles which attenuate and reflect a signal to various degrees. At any given location, the received signal is the sum of many reflected versions of the transmitted signal that propagated along different paths. This alters the amplitude and phase of the received signal. Intersymbol interference is also present due to the different propagation delays of each path. Since the receiver and the surrounding environment tend to be in motion, the channel conditions change with time, making it difficult to estimate the channel state.

A typical multipath channel is characterized by the following impulse response:

$$h(t) = \sum_i a_i(t)\delta(t - T_i(t)) \tag{1.1}$$

or

$$h(t) = \sum_i |a_i(t)|e^{j\theta_i(t)}\delta(t - T_i(t)) \tag{1.2}$$

where $|a_i(t)|$ is the time varying path gain of the ith path, $\theta_i(t)$ is the time varying channel phase of the ith path, and $T_i(t)$ is a set of time varying random delays on the interval $[T_{td}, T_{td} + T_m)$, where T_{td} is the transmission delay and T_m is called the *multipath spread* of the channel.

The *coherence bandwidth of the channel* is given by

$$(\Delta f)_c \approx \frac{1}{T_m} \tag{1.3}$$

where $(\Delta f)_c$ denotes the coherence bandwidth. Any two sinusoids with a frequency separation greater than $(\Delta f)_c$ are affected differently by the channel. Thus, when the coherence bandwidth is small in comparison to the bandwidth of the transmitted signal, the channel is said to be *frequency-selective*. Conversely, if $(\Delta f)_c$ is large compared to the bandwidth of the transmitted signal, the channel is said to be *frequency-nonselective*.

The *Doppler spread*, B_d, is a measure of the rate of change of the set of complex Gaussian random variables $\alpha_i(t)$. The reciprocal of B_d is a measure of the *coherence time* of the channel. This is shown by

$$(\Delta t)_c \approx \frac{1}{B_d} \tag{1.4}$$

where $(\Delta t)_c$ denotes the coherence time. Vehicle velocity and carrier frequency determine this parameter.

The terrestrial mobile channel is discussed in [10,14]. This channel is frequency-selective for DS-CDMA signals and is typically slowly fading with a typical delay spread of 5 microseconds. Figure 1.1 depicts a land mobile communications channel model.

1.2 Thesis Objectives

Direct-sequence CDMA is being considered for cellular and personal communications services for two reasons, to circumvent the lack of available frequency spectrum and to increase current system capacities. The capacity of a DS-CDMA system depends greatly on its bit error rate performance. Since each user acts as interference to all other users, the capacity is determined by the number of simultaneous users the system can support while maintaining an acceptable bit error rate.

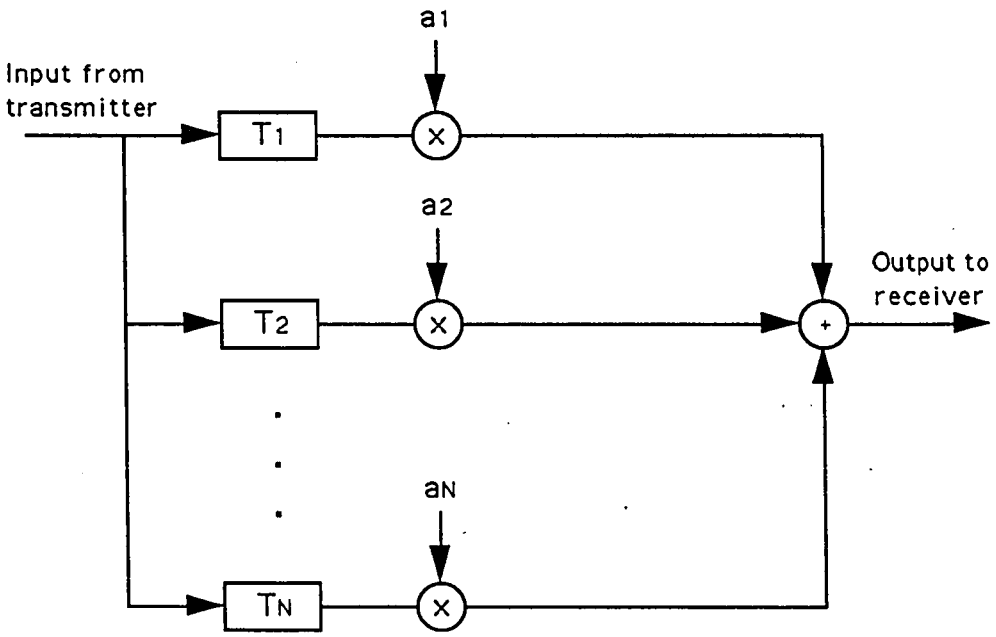

Figure 1.1: Frequency-selective Rayleigh fading channel model.

The objectives of this thesis are:

i) To determine a good DS-CDMA receiver with respect to detection, diversity combining and coding as to maximize the capacity of the system.

ii) To examine these results and to suggest means of further increasing the communication system's capacity.

1.3 Thesis Organization

The remainder of this thesis is organized in five chapters.

Chapter 2 presents a basic explanation of direct-sequence spread spectrum principles. Narrowband interference rejection and multiple access properties are explained in detail.

Chapter 3 reviews previous research and experiments in the field of land mobile communications, the use of spread spectrum, and diversity combining techniques. All experimental procedures, analysis, and results obtained from these experiments are presented.

Chapter 4 discusses diversity combining and detection techniques, as well as the RAKE receiver structures employed in this study. Detailed explanations of each detection scheme and how they are used in conjunction with RAKE receivers are given.

Chapter 5 presents all simulation methods and results. The algorithms used are described in detail and all results are analysed. All detection schemes are compared for a number of channel conditions and coding schemes.

Chapter 6 contains a review of all material presented and renders some conclusions on the performance of certain detection/coding schemes. Based on the results obtained, recommendations for further research are given at the end of the chapter.

Chapter 2

Direct-Sequence Spread Spectrum

Spread spectrum technology, originally developed for military applications where security and resistance to jamming are the critical concerns, requires that a digital signal of limited bandwidth be spread to cover a much larger bandwidth. This technique seems somewhat odd since a typical communications engineer tries to squeeze more and more capacity into as small a bandwidth as possible. However, certain advantages are obtained through the use of direct-sequence spread spectrum. These are [15]:

(1) Protection against jamming and unintentional interference,

(2) Multiple access,

(3) Protection against multipath.

However, certain disadvantages arise when using direct-sequence spread spectrum. The main disadvantages are:

(1) Increase in receiver complexity, and

(1) Inefficient use of channel bandwidth in certain applications.

This chapter provides a detailed explanation of spread spectrum theory needed in the understanding of the concepts presented in this thesis.

2.1 What is Direct-Sequence Spread Spectrum

In direct-sequence spread spectrum [10,16,17,18], a digital signal, $m(t)$, is modulated by a pseudorandom binary code, $c(t)$, known as a *pseudonoise* (PN) code. A pseudonoise code is a string of 1's and 0's which is usually generated at a rate higher than that of the bit stream. These codes are selected for their good autocorrelation properties and their low crosscorrelation with different PN codes. The modulation of the digital signal produces a resultant signal, $s(t) = m(t)c(t)$, which is transmitted. At the receiver, $s(t)$ is modulated with a local replica of the PN code, $c(t)$. Assuming the the local replica of $c(t)$ is aligned with the original, the resultant signal is $m(t)$ since $c^2(t) = 1$. Figure 2.1 demonstrates a direct-sequence spread spectrum signal in both time and frequency domains, where T_b is duration of one bit and T_c is the duration of one chip. A chip is one binary symbol of the PN sequence. Figure 2.2 shows the general form of a direct-sequence spread spectrum communication system.

2.2 Pseudonoise Sequences

The PN sequence is the foundation of direct-sequence spread spectrum. It is this entity which spreads and despreads the information that is transmitted over a spread spectrum system.

A random binary sequence has the following autocorrelation function:

$$R(\tau) = \begin{cases} 1 - \frac{|\tau|}{T_b} & \text{if } |\tau| < T_b \\ 0 & \text{otherwise} \end{cases} \tag{2.1}$$

A pseudonoise sequence is pseudorandom. In other words, it appears random over

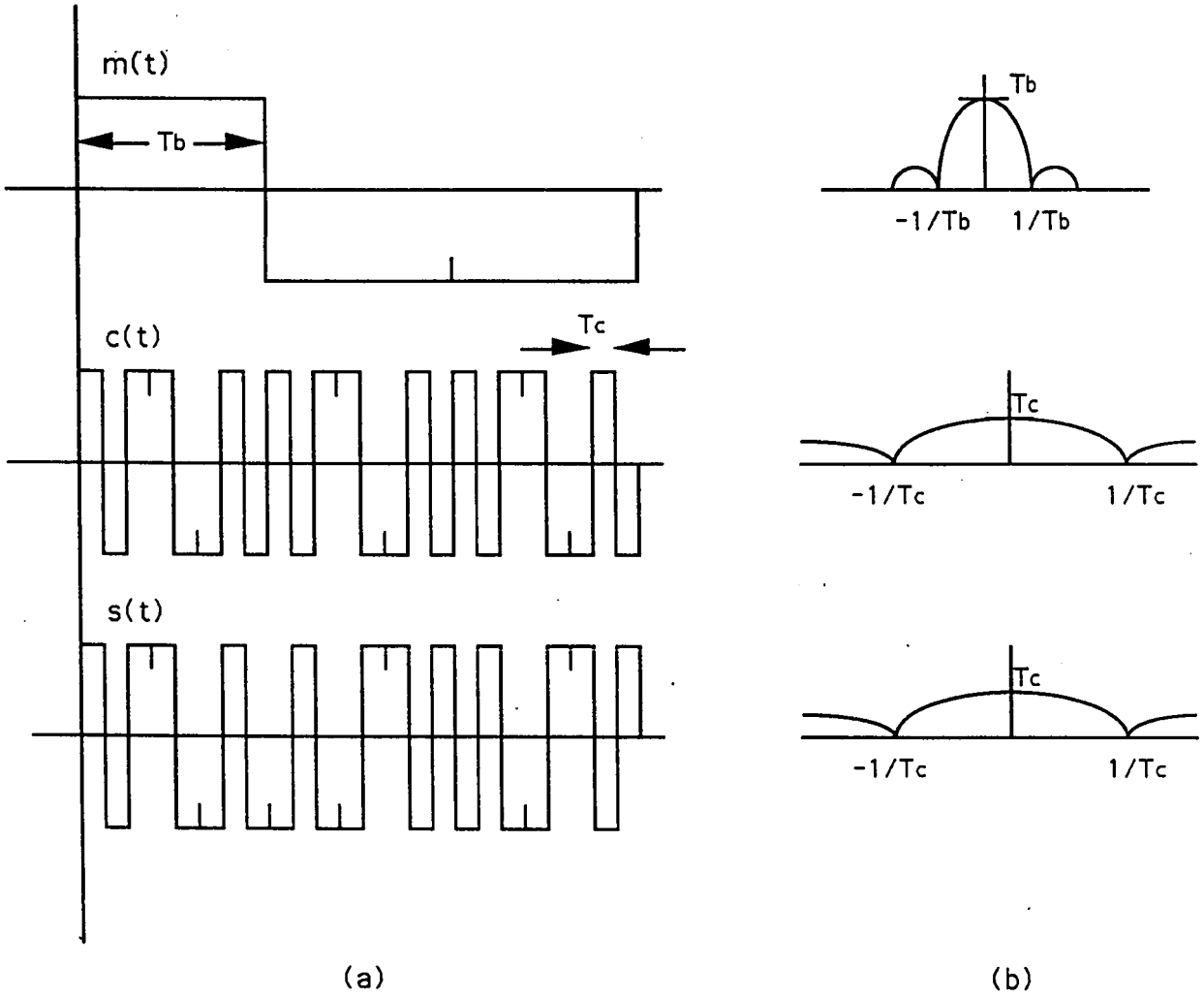

Figure 2.1: Direct-sequence spread spectrum: (a) Time domain (b) Frequency domain.

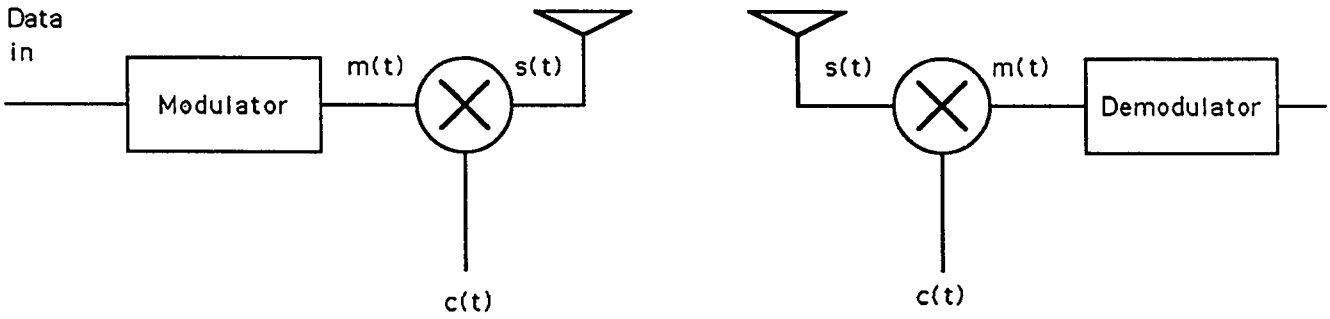

Figure 2.2: A direct-sequence spread spectrum communication system.

some interval of K chips, then it repeats itself. Thus its autocorrelation function is periodic with a period of KT_c where T_c is one chip time. Figure 2.3 demonstrates the autocorrelation function of an ideal PN sequence. From this, one can see that the PN sequences of the transmitter and the receiver must be aligned within one chip in order for the receiver to receive the spread spectrum signal. PN sequence synchronization algorithms exist in order to achieve this. Some PN synchronization schemes are discussed in [19], however they are not discussed in this chapter as some assumptions concerning this aspect of DS spread spectrum are made further on in the thesis.

2.3 Interference Suppression Capabilities of Direct-Sequence Spread Spectrum

Since the advent of spread spectrum, different types of jamming techniques have evolved. These jamming methods include tone or partialband jamming [18,20,21,22], barrage jamming [18] and pulsed jamming [18,21,22]. In commercial systems, however, these types of intentional jamming tend not to occur. Instead, the signal is subjected to unintentional interference from non-spread systems, which is analo-

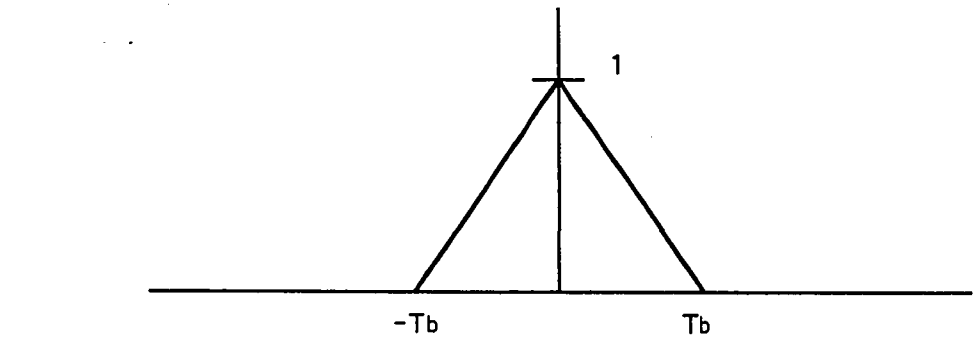

(a)

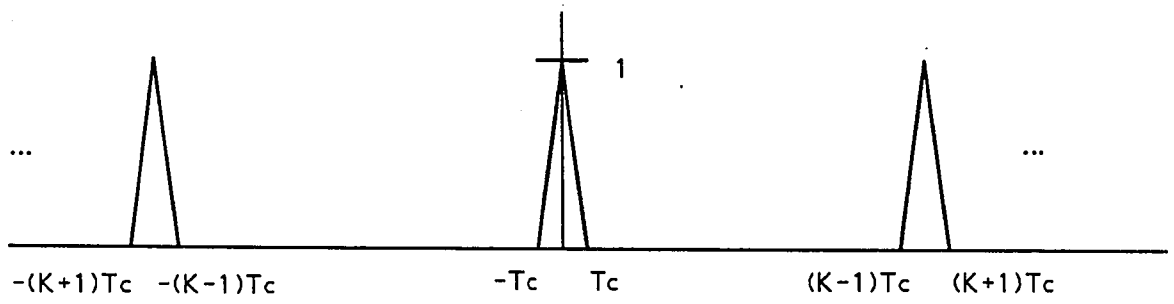

(b)

Figure 2.3: (a) Autocorrelation function of random binary sequence (b) Autocorrelation function of ideal PN sequence.

gous to narrowband jamming. This section will examine only unintentional interference encountered by spectrum sharing with existing users.

Figure 2.4 demonstrates a direct-sequence spread spectrum communication system being acted upon by an interfering signal. Note that while the desired signal is spread at the transmitter and despread at the receiver, the interference signal is modulated by the PN sequence only once. Thus the interference signal is spread over the entire spread bandwidth at the receiver, and this reduces its ability to degrade the performance of the system.

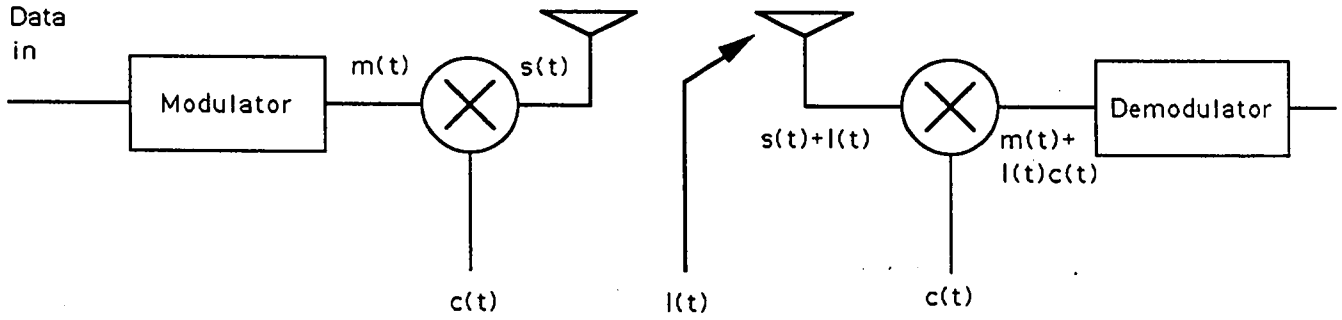

Figure 2.4: Spread spectrum in the presence of interference.

The effect of narrowband interference on a DS-CDMA system is similar to the effect caused by partial band jamming [22]. Consider a DS-CDMA system operating in the same frequency band as a single non-spread system. The power of the non-spread system is denoted as I, its bandwidth as W_{ns}, and its carrier frequency as f_{ns}. The DS-CDMA system has a bit rate denoted by R, a spread bandwidth denoted by W_{ss}, and a carrier frequency given by f_{ss}.

In Figure 2.5 (a), a spread spectrum signal is shown along with a narrowband interference signal. For simplicity, it is assumed that the interference signal's bandwidth, W_{ns}, is extremely small. When the received signal is multiplied by by the local PN sequence, the desired signal is despread, while the interference signal is spread, making it appear to be noise. This is shown in Figure 2.5 (b). The

equivalent interference noise density is denoted as N_i and is approximately [16]:

$$N_i = \frac{I}{W_{ss}} sinc^2[(f_{ss} - f_{ns})T_c] \tag{2.2}$$

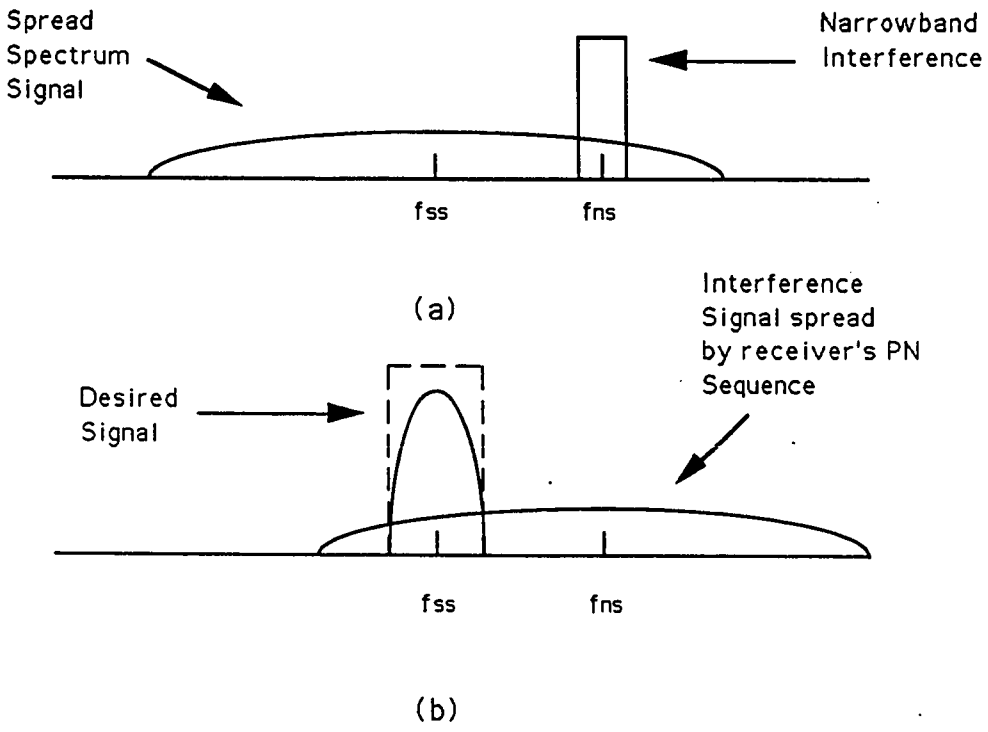

Figure 2.5: Narrowband interference with spread spectrum signal (a) Before despreading (b) After despreading.

When $f_{ss} = f_{ns}$, $N_i = \frac{I}{W_{ss}}$. The equivalent energy per bit to spectral noise density ratio is given by:

$$\frac{E_b}{N_o + N_i} = \left(\frac{E_b}{N_o}^{-1} + \frac{E_b}{N_i}^{-1}\right)^{-1} \tag{2.3}$$

$$= \left(\frac{E_b}{N_o}^{-1} + \left(\frac{E_b W_{ss}}{I sinc^2[(f_{ss} - f_{ns})T_c]}\right)^{-1}\right)^{-1} \tag{2.4}$$

$$= \left(\frac{E_b}{N_o}^{-1} + \frac{I}{C}\frac{R_b}{W_{ss}} sinc^2[(f_{ss} - f_{ns})T_c]\right)^{-1} \tag{2.5}$$

where $C = E_b/R_b$ and is the total signal power.

Figure 2.6 shows the effect of narrowband interference on a DS-CDMA signal with an energy per bit to spectral noise density ratio, E_b/N_o, of 10dB for different spreading factors. The center frequencies of both the CDMA signal and the narrowband interference are equal in this figure.

In the case where many non-spread systems exist within the DS-CDMA system's bandwidth, the equivalent interference noise density becomes:

$$N_{i\ eq} = \frac{I_1}{W_{ss}} sinc^2[(f_{ss} - f_{ns1})T_c] + \frac{I_2}{W_{ss}} sinc^2[(f_{ss} - f_{ns2})T_c] \ldots \tag{2.6}$$

2.4 Multiple Access

Multiple access is obtained in a DS-CDMA network by assigning each user a different PN sequence. Since a transmitted signal can only be despread by the correct PN sequence, the signal remains spread when it is received by a user for which the signal is not intended. Assuming that the transmissions are asynchronous, undesired signals appear similar to interference and can be approximated by white noise. This multi-user interference is known as *mutual interference* [8]. As the number of additional users to the communication system increases, the performance of each individual user degrades. Thus, the capacity of a DS-CDMA communication

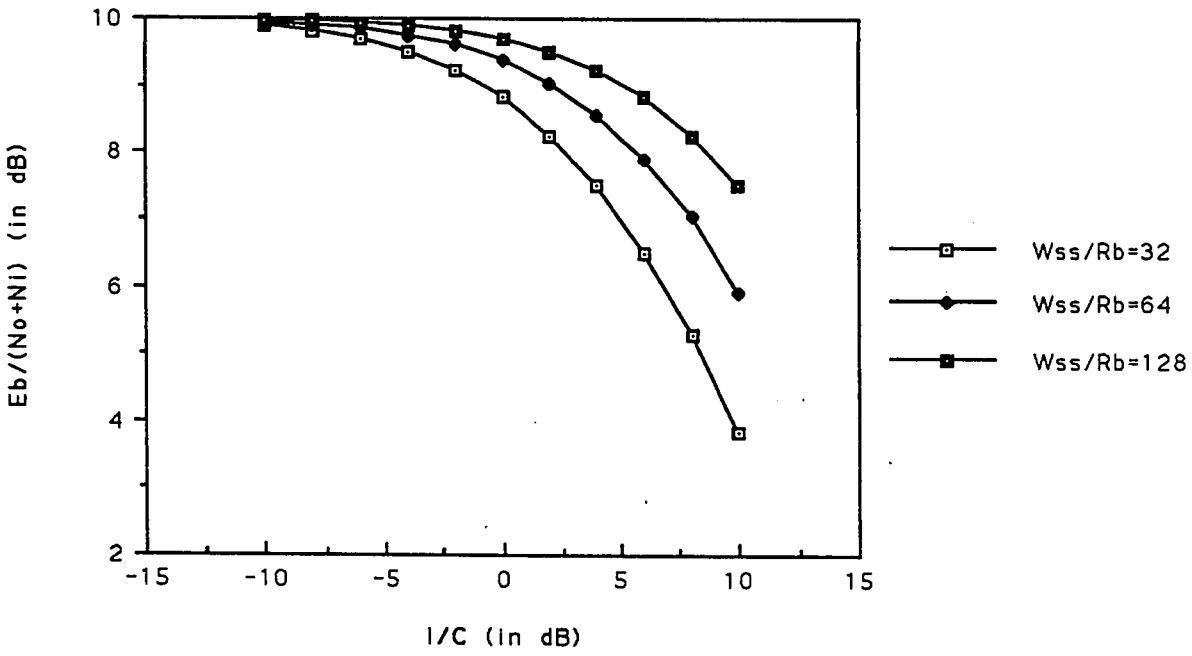

Figure 2.6: Effect of narrowband interference on a DS-CDMA system for different spreading factors. ($E_b/N_o = 10dB$, $f_{ss} = f_{ns}$).

system is limited by the maximum number of simultaneous users allowable while maintaining an acceptable bit error rate performance.

The following analysis of mutual interference is presented in [8] and is often accepted as being an accurate estimate of the performance degradation due to simultaneous users in a spread spectrum system.

Suppose M users are transmitting direct-sequence spread spectrum signals such that the received signals all have the same power. Let there be a single hub station with receivers for all users.

The received noise power is the sum of the thermal noise, $N_o W_{ss}$ and the interference from the other $M-1$ users, where W_{ss} is the bandwidth of the spread spectrum signal. Since the interferers will be at a random phase relative to the others, the received interfering power from the $M-1$ users is $(M-1)E_c/T_c$, where E_c is the received energy in one chip and T_c is the chip duration. The equivalent received noise power is

$$N_o' W_{ss} = N_o W_{ss} + (M-1)E_c/T_c \tag{2.7}$$

and therefore the equivalent spectral noise density is

$$N_o' = N_o + (M-1)E_c \tag{2.8}$$

since $W_{ss}T_c = 1$. From this expression for the spectral noise density, the effective signal energy per chip to spectral noise density ratio is given by

$$\frac{E_c}{N_o'} = \frac{E_c/N_o}{1 + (M-1)E_c/N_o} \tag{2.9}$$

The spreading factor is expressed in chips per bit, and is given by

$$B_c = R_c/R_b \quad (2.10)$$
$$= W_{ss}/R_b \quad (2.11)$$

where R_c is the chip rate and R_b is the bit rate. The received energy per bit, E_b can be expressed as $B_c E_c$, therefore

$$\frac{E_b}{N_o'} = \frac{E_b/N_o}{1 + (M-1)(1/B_c)(E_b/N_o)} \quad (2.12)$$

Figure 2.7 demonstrates the effect of mutual interference on the effective energy per bit to spectral noise density ratio, E_b/N_o', for a single user energy per bit to spectral noise density ratio, E_b/N_o, equal to 10dB.

2.5 DS-CDMA System Capacity

Equation (2.12) gives an expression for the effective energy per bit to spectral noise density ratio, E_b/N_o'. This quantity determines the bit error performance of the communication system. In order to communicate effectively, it is required that the bit error rate not exceed a certain value (for voice communication, BER $\leq 10^{-3}$). Therefore, E_b/N_o' has a minimum value, γ'. When $E_b/N_o' = \gamma'$, a maximum number of user is achieved. Therefore $M = M_{max}$. Inserting these quantities into Equation (2.12) yields

$$\gamma' = \frac{E_b/N_o}{1 + (M_{max}-1)(1/B_c)(E_b/N_o)} \quad (2.13)$$

Rearranging Equation (2.13) to give an expression for M_{max} yields the following

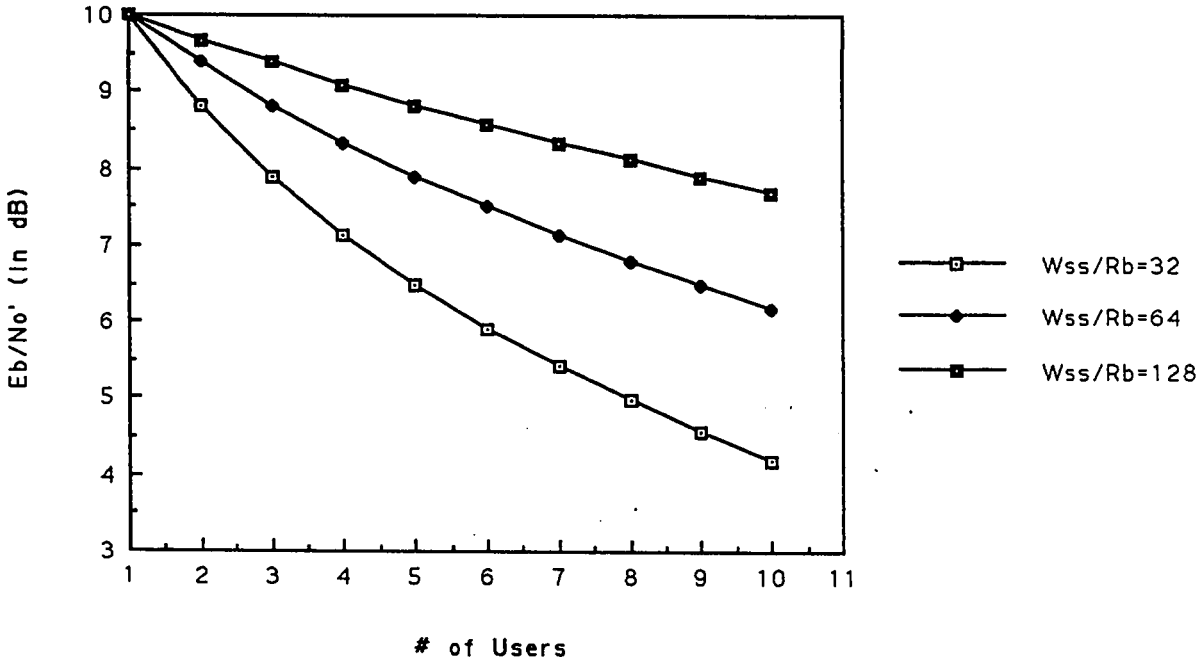

Figure 2.7: Effect of mutual interference on the effective E_b/N_o' for different spreading factors. ($E_b/N_o = 10$dB).

$$M_{max} = \frac{E_b/N_o - \gamma' + (1/B_c)(E_b/N_o)(\gamma')}{(1/B_c)(E_b/N_o)(\gamma')} \quad (2.14)$$

The spectral efficiency, η, of a communication system is measured in the number of bits per second transmitted over the bandwidth employed. Therefore, this is determined by $M_{max}R_b/W_{ss}$ which is equal to M_{max}/B_c. The spectral efficiency, η, of a DS-CDMA communications system is given by

$$\eta = \frac{E_b/N_o - \gamma' + (1/B_c)(E_b/N_o)(\gamma')}{(E_b/N_o)(\gamma')} \quad (2.15)$$

When B_c is large, η becomes

$$\eta = \frac{E_b/N_o - \gamma'}{(E_b/N_o)(\gamma')} \quad (2.16)$$

As E_b/N_o becomes large, the spectral efficiency is expressed as

$$\eta = \frac{1}{\gamma'} \quad (2.17)$$

Figure 2.8 shows the spectral efficiency of a DS-CDMA system for different values of γ'. It can be seen that the capacity of the channel increases as γ' decreases. This figure shows the need for the optimization of a DS-CDMA system.

2.6 Power Control

The expressions in the two previous sections were derived under the assumption that the received signal from each user was equal in power to the others. Indeed,

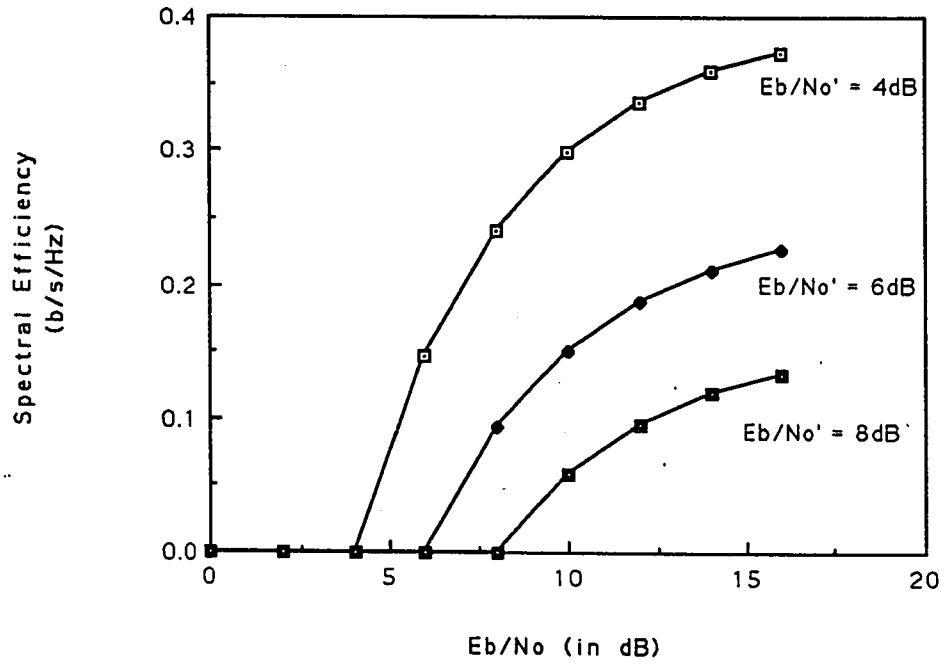

Figure 2.8: Spectral efficiency of a DS-CDMA communications system.

if one user's signal is received with a much higher power than the others, the capacity of the system will decrease since the system is power limited. This is demonstrated in [18]. Therefore, in order to maximize the capacity of a DS-CDMA communication network, power control is essential.

Perfect power control is assumed in most papers concerning DS-CDMA as well as in this thesis. Opponents of CDMA claim that the need for power control makes CDMA undesirable. However, Qualcomm has developed a power control algorithm which can control the transmitted power from each mobile so that the corresponding received power at the base station is maintained within a standard deviation of $\pm$ 1.5dB [23].

2.7 Voice Activity

When using DS-CDMA for voice transmission, the statistics of voice activity can be exploited. When a user's terminal is in use, about 35% of the time is spent talking [6]. By transmitting a signal only when the user is actually talking, decreases the mutual interference in the channel when she is listening. Thus, more users can access the channel when the voice activity factor is exploited. Therefore, the capacity of the channel becomes

$$\eta = \frac{E_b/N_o - \gamma'}{V(E_b/N_o)(\gamma')} \tag{2.18}$$

where V is the voice activity factor.

Figure 2.9 demonstrates the increase in the channel capacity due to the voice activity factor.

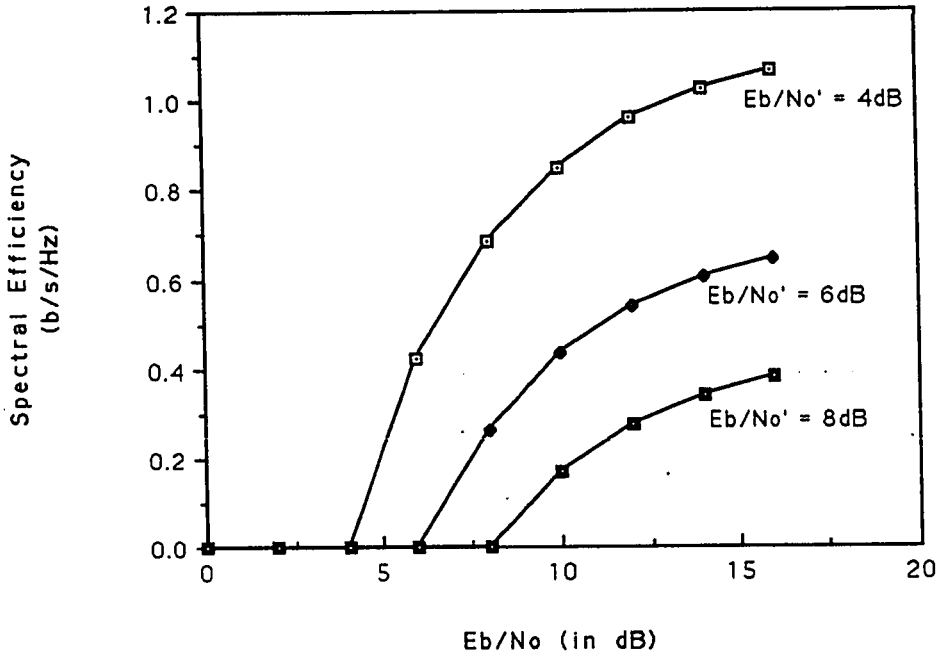

Figure 2.9: Spectral efficiency of a DS-CDMA communications system for a voice activity factor of 35%.

2.8 Error Control Coding

By applying forward error correction coding to the information stream, the bit error performance of the DS-CDMA system can be improved, thus lowering γ', and in turn increasing the capacity of the communication system. However, it would appear that the use of coding, which increases the symbol rate, will decrease the spreading factor of the DS-CDMA system. While there is an actual physical spreading reduction due to the increase in channel symbols, the effective spreading factor remains unchanged [23].

When coding is used, the energy per coded symbol is E_{cs} and the coded symbol rate is R_{cs}. These values are inserted into Equation (2.12).

$$\frac{E_{cs}}{N_o'} = \frac{E_{cs}/N_o}{1 + (M-1)(R_{cs}/R_c)(E_{cs}/N_o)} \tag{2.19}$$

However, $E_{cs} = rE_b$ and $R_{cs} = R_b/r$ where r is the code rate and is a measure of redundancy brought on by the coding process. Therefore Equation (2.19) becomes

$$\frac{E_{cs}}{N_o'} = \frac{E_{cs}/N_o}{1 + (M-1)(R_b/rR_c)(rE_b/N_o)} \tag{2.20}$$

$$= \frac{E_{cs}/N_o}{1 + (M-1)(R_b/R_c)(E_b/N_o)} \tag{2.21}$$

It can be seen from Equation (2.21) that the increase in the spectral noise density is the same as in the uncoded case, therefore the effective spreading factor remains unchanged when coding is added.

2.9 Summary

This chapter provided a brief tutorial on DS-CDMA concepts needed in the understanding of this thesis. The following points were presented:

1) A direct-sequence spread spectrum signal is produced by modulating a digital signal by a pseudorandom binary sequence known as a pseudonoise (PN) sequence.

2) Direct-sequence spread spectrum technique is extremely effective for the suppression of narrowband interference.

3) By using a different PN sequence for each user, multiple access is made possible by direct-sequence spread spectrum. This is known as direct-sequence code division multiple access (DS-CDMA).

4) DS-CDMA network capacities are power limited rather than bandwidth limited.

5) Good power control is required in order to maximize the capacity of a DS-CDMA system.

6) The capacity of a DS-CDMA system can be increased by the exploitation of the voice activity factor.

7) Coding does not affect the effective spreading factor of a DS-CDMA system. Thus coding increases the capacity of a DS-CDMA system by lowering γ'.

Chapter 3

Review of Previous Research

Direct-sequence code division multiple access (DS-CDMA) for mobile radio has been one of the main topics under investigation in recent years. Previous research has found it to be an efficient solution in the suppression of multipath and the increasing of channel capacities. This chapter focuses on the research done in the field of DS-CDMA and fading channels.

This chapter is divided into two sections. The first section deals with previous research of the use of DS-CDMA over fading channels. The research discussed in this section deals with diversity reception of frequency-selective Rayleigh faded signals obtained through direct-sequence spread spectrum. The second section concentrates on different detection schemes for fading channels. Different papers on the use of multiple symbol differential detection and coherent detection are discussed in this section.

3.1 DS-CDMA for Fading Channels

The performance of digital radio in harsh frequency-selective Rayleigh fading environments is extremely poor. The interference rejection properties of direct-sequence spread spectrum allows it to suppress all multipath components that

are not synchronized to the receiver's PN sequence. This ability to isolate one single path from the overall received signal allows a DS spread spectrum receiver to isolate all multipath components by the use of a RAKE receiver.

One of the most influential research papers on this subject is presented by Turin [24]. Using a channel model which he derives from literature and experimentation [14], Turin presents analytical results for the optimal single path receiver (frequency-nonselective) and the optimal multipath receiver. In the case of the optimal multipath receiver, an ideal RAKE receiver with apriori knowledge of the path delays and the path strengths is considered. Differential binary-phase-shift-keying (DBPSK) modulation is assumed throughout this study.

At this point, Turin suggests channel sounding receivers as a means of providing the RAKE receiver with reliable path delay estimates. The knowledge of the path delays is crucial as it allows the receiver to switch off any RAKE taps which do not contain any information. This will be discussed further in the next chapter.

Incorporating a sounding receiver into the overall RAKE receiver (a structure which Turin refers to as a digital RAKE), Turin performs simulations by assuming that the sounding receiver's path delay estimates are exact. From these simulations, Turin concludes that the digital RAKE performs within 1dB of the ideal RAKE receiver for low rate transmissions. For high rate transmissions, the digital RAKE performs within 2.5dB of the ideal RAKE.

Turin elaborates on this study in a later paper [25], where he investigates the effects of the channel on the capacity of a DS-CDMA communication system. He first calculates the spectral efficiency of a DS-CDMA communication system in an AWGN channel for DBPSK modulation. He then calculates the spectral efficiency of a DS-CDMA system with RAKE reception which encounters frequency-selective Rayleigh fading. He finds that the spectral efficiency of the latter situation decreases by a factor of 5 in dense urban areas as compared to the spectral efficiency in an AWGN channel. In suburban areas, the capacity decreases by as much as a factor of 24. This is due to the fact that in suburban areas, there is usually one strong faded path and thus multipath diversity is not available to overcome the interference from other users.

He assumes that the transmitted powers of all users are fixed, and because of this,

the signals from different users arrive with different signal strengths. Therefore, he concludes that a form of power control is needed in order to improve the spectral efficiency of a DS-CDMA system when fading is present. His results do not take error control coding or voice activity into account.

In 1987, Kavehrad and Ramamurthi [26] obtain the performance of DS-CDMA with DPSK modulation and diversity for indoor wireless channels. The matched filter based receiver employs a surface acoustic wave (SAW) device. The SAW device is matched to the PN sequence of each specific user. This is further explained in a previous paper by Kavehrad and McLane [27].

In [26], Kavehrad and Ramamurthi compare their DPSK receiver to the coherent PSK receiver discussed in [27]. They determine the performance through numerical analysis as well as through Monte Carlo simulations. They conclude that the system with DPSK modulation compares well to the coherent PSK system. They find that the power penalty at low values of E_b/N_o is about 4dB for the DPSK system, and the increase in the irreducible error floor compared to that of coherent PSK is less than half an order of magnitude. However, their conclusions do make a case for the use of coherent detection since a 4dB gain represents a huge gain in capacity for DS-CDMA systems. These results do not consider forward error correction.

Oschner [28] provides some numerical analysis of an optimum non-coherent direct-sequence spread spectrum receiver for frequency-selective Rayleigh fading channels. In his analysis, some assumptions are made. Firstly, he assumes that the channel is time-invariant over a symbol duration. This assumption is generally accepted when slow fading is considered. Secondly, he assumes PN sequences with ideal autocorrelation properties so that multipath components do not interfere with each other at the receiver. His receiver also has an a priori knowledge of the path gains.

His results show that RAKE reception provides huge gains over conventional spread spectrum reception (non-diversity), however, even when the order of diversity is great, the results do not approach those for a nonfading channel. Therefore, he demonstrates that the capacity of a DS-CDMA system decreases when fading is present, even when the diversity is exploited.

Lam and Steele [29] demonstrate the diversity reception of frequency-selective Rayleigh fading by a coherent direct-sequence spread spectrum RAKE receiver. Their results are obtained through computer simulation of their system model. The coherent detection is obtained by interleaving a sounding sequence into the data stream to allow the receiver to estimate the channel impulse response. No forward error correction is considered.

For the system that they consider, the number of simultaneous users is small. They conclude that the performance of the system depends heavily on the nature of the channel, especially the number of resolvable paths. In other words, as the number of resolvable paths increases, thus increasing the order of diversity, the performance improves. They also conclude that the performance is improved by increasing the spreading rate at the price of employing more spectrum. This conclusion is obvious. By increasing the spreading factor, the number of resolvable paths increases and the interference from each path to the others decreases. However, this is not the best solution to their problem. Error control coding should improve the performance of the single user, thus increasing the capacity of the system without increasing the bandwidth.

All of the papers presented in this section demonstrate that the capacity of a DS-CDMA communication system decreases when fading is present as opposed to the classical AWGN channel. However, the use of DS-CDMA along with a RAKE receiver is still an effective method at combatting multipath. Its ability to employ low rate codes without penalty, its ability to exploit voice activity, and the greater frequency reuse obtained by DS-CDMA are some reasons why DS-CDMA continues to draw so much attention.

3.2 Detection Schemes for Fading Channels

The capacity of a DS-CDMA system is directly proportional to its single user bit error rate performance. Developing detection schemes which improve the bit error performance of the communication system, allows the tolerance to interference to increase, thus allowing the number of simultaneous users to increase.

In the previous section, differential detection was the detection scheme employed by most researchers. This is due to the fact that differential detection relies only on the relative phase between two consecutive bits, therefore the channel phase of a slowly fading channel need not be determined. However, it is shown in [10] that coherent detection provides a theoretical 3dB gain over differential detection in frequency-nonselective Rayleigh fading channels. Therefore, it would be beneficial to the capacity of a DS-CDMA communication system to attempt to approximate coherent detection in a fading channel.

Multiple symbol differential detection (MSDD) is a detection scheme considered by Divsalar and Simon [12]. This detection scheme observes the phase change over a number of symbol intervals in its determination of the transmitted symbol. Maximum likelihood sequence estimation is the decision rule in determining the proper transmitted symbol.

They analyse the receiver numerically in order to determine the bit error performance of this receiver in an AWGN channel. As they increase the detection window (observation period) to include more symbols, the performance of MSDD tends towards the bit error probability of coherent detection. Therefore, they show that it is possible to obtain the bit error performance of coherent detection without employing a coherent detector. It is shown that a detection window of 5 bits is extremely close to the coherent detection performance bound. However, it should be noted that a multiple symbol differential detection receiver with a detection window of 5 is extremely complex when compared to conventional differential detection.

It is important to note that the results obtained by Divsalar and Simon are for AWGN channels. However, for frequency-nonselective slowly Rayleigh fading channels, these results might also apply.

Multiple symbol differential detection does approach the performance of coherent detection but at the cost of increased complexity. Other researchers have investigated the possibility of implementing coherent detection in mobile communications by sounding the channel. Davarian [30] analyses a system which employs a continuous-wave (CW) tone to calibrate the mobile channel against multipath-induced phase uncertainties. In his system, the relative position of the tone is care-

fully selected so that the tone and signal experience the same distortion. Secondly, the tone coincides in frequency and phase with the carrier in order to obtain coherent demodulation. Finally, the tone uses only a small portion of the total power. A spectral null is created at the tone's position in order to avoid self-interference. This is done by employing one of many schemes of encoding the data so that the DC component is suppressed.

Davarian's analysis of this receiver shows that the bit error performance is comparable to ideal PSK in the presence of frequency-nonselective Rayleigh fading, with the performance depending on the amount of power allocated to the pilot. In the presence of Rician fading, the receiver also performs quite well compared to ideal PSK. Davarian concludes that this technique is suitable for digital communications over mobile channels for the reasons that it is very robust, it performs well for low bit rate communications in fast fading channels, and that it has good power and spectral properties.

Another method of coherent detection over fading channels is discussed by Moher and Lodge [31]. In their paper, they discuss the transmission of trellis coded modulation (TCM) which maps the output of a convolutional encoder to various voltage levels. The resultant signal is a pulse amplitude modulation signal, which is extremely vulnerable to the fading nature of the channel as the information is carried in both the phase and the amplitude. Therefore it is very important to estimate the channel phase and gain. Tone calibration discussed by Davarian would be one possible method, however, Moher and Lodge decided to interleave pilot symbols within the actual data stream. This is known as pilot symbol-aided detection. The pilot symbols are extracted from the data stream at the receiver. They are then used to estimate the channel phase and gain. Therefore, the effects of the channel can be compensated for at the receiver.

Using computer simulation, Moher and Lodge examine the performance of this system over a Rician channel. They conclude that their pilot symbol-aided trellis coded modulation scheme provides a robust performance over a wide range of Rician fading channels. They show that a code of relatively modest coding gain and complexity can provide substantial improvements over uncoded schemes.

Three different detection schemes have been presented in this section. Multiple

symbol differential detection has been shown by Divsalar and Simon to approximate the performance of coherent detection while Davarian's tone calibration system allows for coherent demodulation of the signal and performs slightly worse than ideal PSK in fading channels. All methods have been shown to improve performance of a digital communication system in the presence of fading. This is extremely desirable in a DS-CDMA communication system where the performance of the system can be traded off against capacity.

Chapter 4

Diversity Combining and RAKE Receivers

In a diversity system, the receiver obtains several copies of the same message through several different channels. This can be done intentionally, where the transmitter sends the message a number of times, either by time diversity or frequency diversity. The receiver may employ many receivers in obtaining a single copy of the transmitted signal. This is known as site diversity. Diversity can also be obtained unintentionally, where the transmitter sends a single signal and reflections from objects in the environment create differently faded versions of the signal.

In each case, it is the receiver's task to utilise each received copy of the signal in its determination of the transmitted signal. The act of combining different copies of the received signal is known as *diversity combining.*

4.1 Diversity Combining

This section discusses different type of diversity combining systems. These are:

1) Hard decision diversity combining,

2) Selection diversity combining,

3) Maximal-ratio diversity combining,

4) Square-law diversity combining,

5) Equal-gain diversity combining.

4.1.1 Hard Decision Diversity Combining

Hard decision diversity [32] behaves exactly like a hard decision decoded repetition code. A decision is made on all of the L channel outputs. The receiver then verifies each decision and chooses the symbol which has been selected most often. Assuming binary signalling and that each diversity path has the same probability of bit error p_b, a bit error would occur only when more than half of the diversity paths are in error. Assuming that all diversity paths are independent and that their number, L, is odd, the probability of bit error, $p_b(L)$, of this diversity combining system is:

$$p_b(L) = \sum_{l=(L+1)/2}^{L} \binom{L}{l} p_b^l (1-p_b)^{L-l} \tag{4.1}$$

4.1.2 Selection Diversity Combining

A selection diversity [33] receiver observes the average power of each diversity path and demodulates only the path with the highest average power, the others do not contribute. Figure 4.1 demonstrates a selection diversity receiver.

Brennan [33] demonstrates the increase in effective average power as a function of diversity order, $P_{av}(L)$, when selection diversity is used.

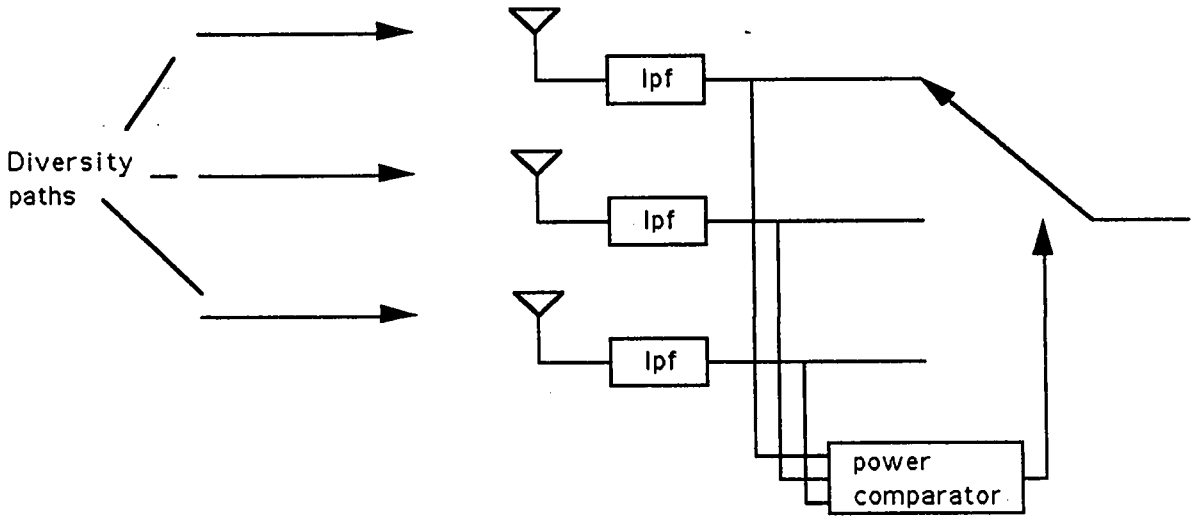

Figure 4.1: Selection diversity combining receiver.

$$P_{av}(L) = P\sum_{k=1}^{L}\frac{1}{k} \tag{4.2}$$

where P is the average power of a single diversity path. Thus $P_{av}(2) = \frac{3}{2}P$, $P_{av}(3) = \frac{11}{6}P$.

4.1.3 Maximal-Gain Diversity Combining

Maximal-gain diversity is the optimum diversity combining law for coherent detection [33]. In other words, after the diversity paths are combined, the resultant signal has the maximum possible signal to noise ratio. This is done by weighting each path before the paths are combined. This is demonstrated in Figure 4.2 where w_1, w_2, w_3 are the weighting factors for each diversity path.

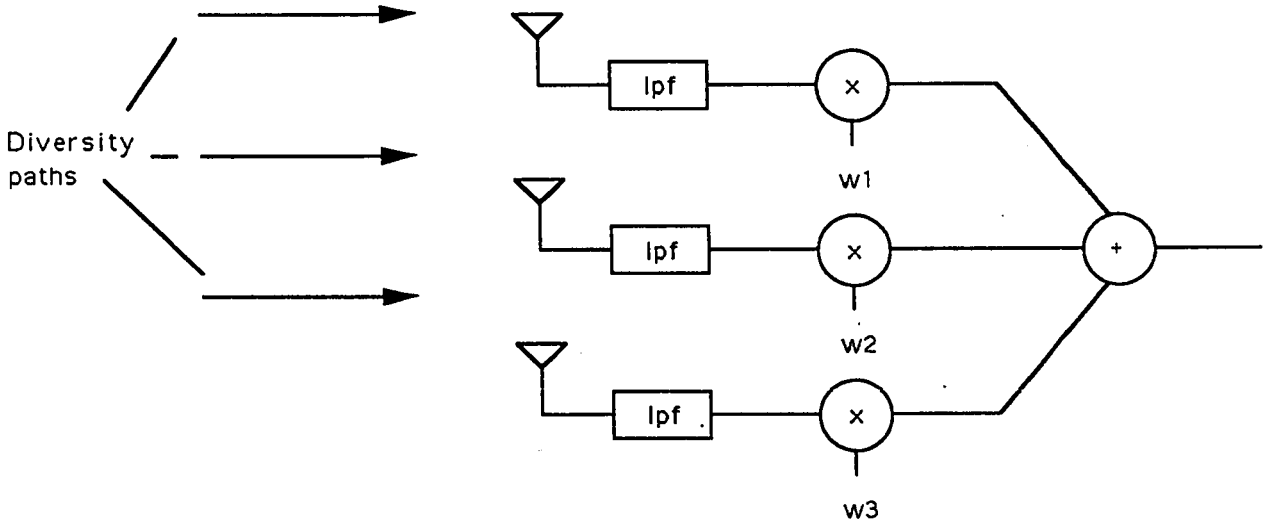

Figure 4.2: Maximal-gain diversity combining receiver.

Consider a two path diversity system. Assume that each path contains the same transmitted power. Let a_1 be the channel gain of path 1, and let a_2 be the channel gain of path 2. Let both paths encounter the same noise density, N_o. At the receiver, path 1 is weighted by w_1 and path 2 is weighted by w_2. Since the actual information is added coherently and the resultant noise is added incoherently, the equivalent energy per bit to noise density ratio, $(E_b/N_o)_{eq}$ is

$$\left(\frac{E_b}{N_o}\right)_{eq} = \frac{(a_1w_1 + a_2w_2)^2 E_b}{(w_1^2 + w_2^2)N_o} \tag{4.3}$$

The equivalent energy per bit to spectral noise density, $(E_b/N_o)_{eq}$, is maximized by maximizing equation (4.3). It can be shown that this equation is maximized by setting $w_1 = a_1$ and $w_2 = a_2$.

In the case of fading channels, a channel phase must also be considered. Therefore the weighting factor, w_i must correct the phase as well. Therefore $w_i = |a_i|e^{-j\theta}$, where θ is the channel phase.

When this is the case, equation (4.3) becomes

$$\left(\frac{E_b}{N_o}\right)_{eq} = (a_1|^2 + |a_2|^2)\frac{E_b}{N_o} \tag{4.4}$$

Therefore, for an Lth order diversity combining system,

$$\left(\frac{E_b}{N_o}\right)_{eq} = \sum_{k=1}^{L} |a_k|^2 \frac{E_b}{N_o} \tag{4.5}$$

In order to determine the performance of this diversity combining system, the probability density function of $(E_b/N_o)_{eq}$ must be determined. If Rayleigh fading is assumed, then $|a_k|$ is Rayleigh distributed and $|a_k|^2$ has a Chi-Square distribution.

The probability density function of $(E_b/N_o)_{eq}$ as a function of the diversity order L is given in [10] as

$$p\left(\frac{E_b}{N_{o\,eq}}\right) = \frac{1}{(L-1)!\bar{\gamma}_c}\left(\frac{E_b}{N_{o\,eq}}\right)^{L-1} e^{-\frac{(E_b/N_o)_{eq}}{\bar{\gamma}_c}} \tag{4.6}$$

where $\bar{\gamma}_c$ is the average E_b/N_o per channel. In other words, $\bar{\gamma}_c = (E_b/N_o)_{eq}/L$.

By averaging the probability of error over this distribution, the bit error probability, $p_b(L)$ can be found to be [10]

$$P_b(L) = \left(\frac{1-\mu}{2}\right)^L \sum_{k=0}^{L-1} \binom{L-1+k}{k} \left(\frac{1+\mu}{2}\right)^k \tag{4.7}$$

where $\mu = \sqrt{\frac{\bar{\gamma}_c}{1+\bar{\gamma}_c}}$.

4.1.4 Square-Law Diversity Combining

Maximal-gain diversity combining is so named because the weighting of the paths provides the maximum possible signal to noise ratio at the combiner. However, this technique requires knowledge of the channel gain and phase. For non-coherent communications, such as FSK, where phase is not important, square-law diversity combining is a means of approximating maximal-gain diversity combining.

In square-law diversity combining [35], each path is squared before being combined with the other paths. Thus the channel gain is squared as in maximal-gain ratio combining, but noisy components are squared as well.

The performance of a binary FSK diversity combining system which employs square-law diversity is discussed in [10]. The expression for the bit error probability is the same as in equation (4.7) with the exception that $\mu = \frac{\bar{\gamma}_c}{2+\bar{\gamma}_c}$.

4.1.5 Equal-Gain Diversity Combining

In equal gain combining [36], each path is received and summed with the other paths without being weighted. This is equivalent to maximal-gain combining when the channel gains are all equal to 1.

An interesting case of this diversity combining method is when it is used with DPSK in Rayleigh fading. In this case, the output of the differential detectors are summed together, however, this behaves much like square-law diversity since the current symbol is multiplied by the previous symbol in the detection process.

This diversity method with DBPSK is analysed in [10]. The bit error probability of this system is the same as equation (4.7) with the exception that $\mu = \frac{\bar{\gamma}_c}{1+\bar{\gamma}_c}$.

4.2 RAKE Receivers

RAKE receivers were first discussed in 1958 by Price and Green [34]. This receiver employs a single delay line through which the received signal is passed. The signal on each tap is demodulated and combined in order to increase the equivalent signal to noise ratio. Figure 4.3 demonstrates this receiver structure.

The structure given in Figure 4.3 can be modified in order to allow the use of spread spectrum. The RAKE receiver will have a tap for each chip in the pseudonoise sequence with each delay on the tapped delay line being equal to one chip time. By including a despreader on each tap, each independent path can be received. Figure 4.4 shows the receiver structure after this modification.

Since most taps will contain only noise, it is important to eliminate these taps from contributing to the output. Consider a system which transmits 10 kbps using a PN sequence that is 128 chips long that is repeated every information bit. Knowing that T_m is typically 5 microseconds, and a chip time is slightly less than 1 microsecond, all information from the channel will be received on about 7 adjacent taps. Algorithms allowing 7 or less adjacent taps with the highest average power is one method of eliminating all other noisy taps.

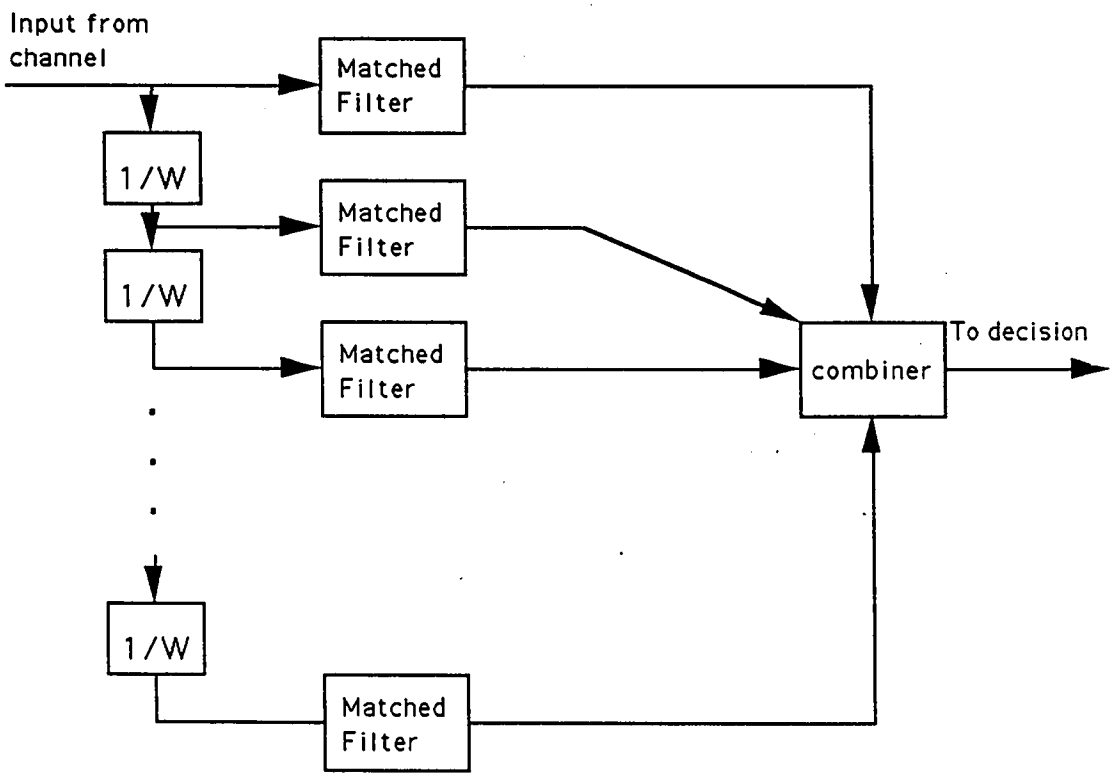

Figure 4.3: Price and Green's RAKE receiver.

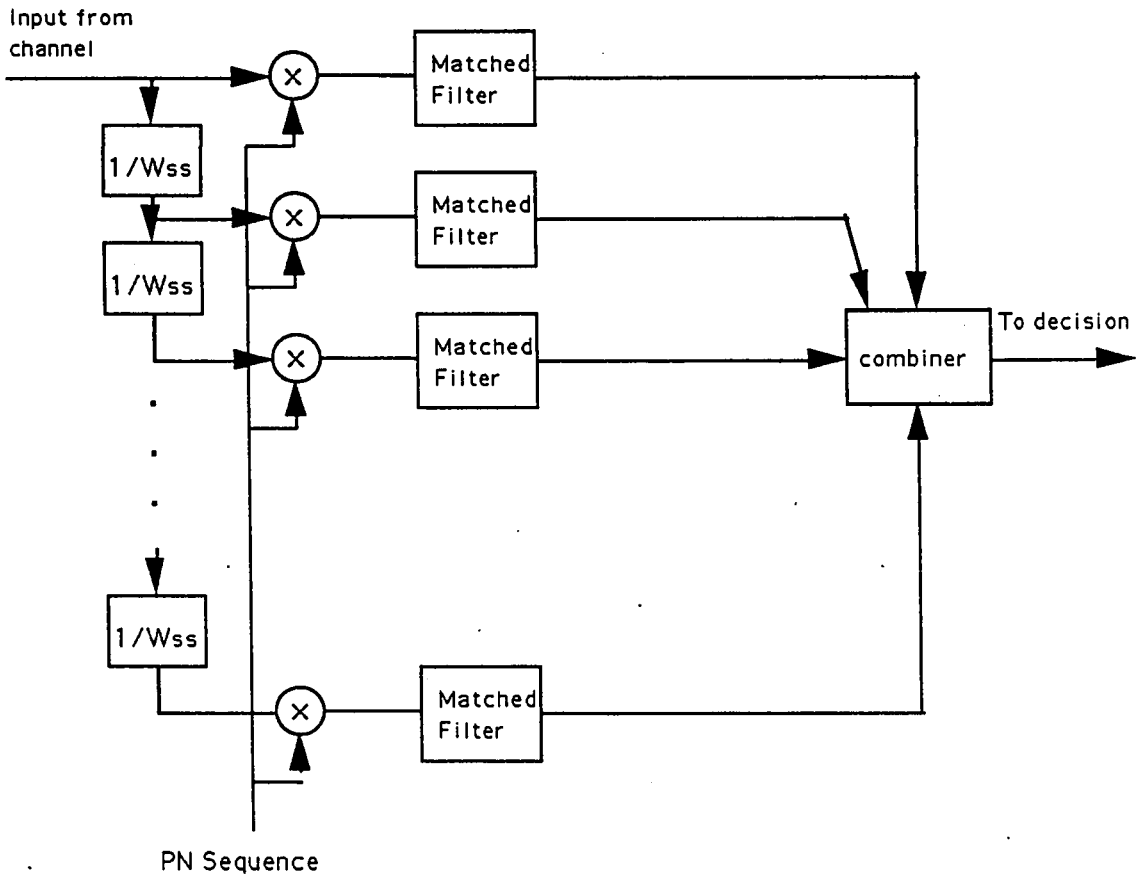

Figure 4.4: A direct-sequence spread spectrum RAKE receiver.

Sounding the channel [24] is another method of noisy tap elimination. In this method, a sounding signal is sent within the transmitted data stream or by itself. This signal is received and processed by a nonlinearity. The output of this nonlinearity contains spikes corresponding to the delays of each path. The receiver then activates the taps which correspond to these delays. This method is used when delay spreads are large, and paths are not received on adjacent paths.

4.2.1 Differential RAKE Receiver

Differential detection is clearly the simplest choice as it was conceived for this type of channel. Although the optimum combining law is not known, the simplest approach appears in [10] which uses equal gain diversity combining. Because each received bit is multiplied by the previous received bit in differential detection, equal gain combination of the outputs of numerous differential detectors behaves like square-law combining. Therefore, this is a close approximation to maximal-gain diversity combining. The structure of the differential RAKE receiver with equal gain combining is shown in Figure 4.5.

4.2.2 Pilot Symbol-Aided Coherent Detection RAKE Receiver

By interleaving a pilot sequence within the channel symbols [31,35], it is possible to sound the channel in order to estimate the channel phase. The pilot symbols also provide power estimates needed for maximal-gain diversity combining.

At the receiver, the pilot symbols are stripped away from the channel symbols to be used to estimate the path gain and phase. Delaying the channel symbols by the appropriate amount, channel prediction can be performed with a smoothing filter rather than a prediction filter. The pilot symbols are interpolated and are fed to the smoothing filter which has a bandwidth slightly larger than the fading bandwidth of the channel. The pilot symbols appear as nearly continuous to this filter and more noise can be removed. Figure 4.6 depicts a pilot symbol-aided coherent RAKE receiver .

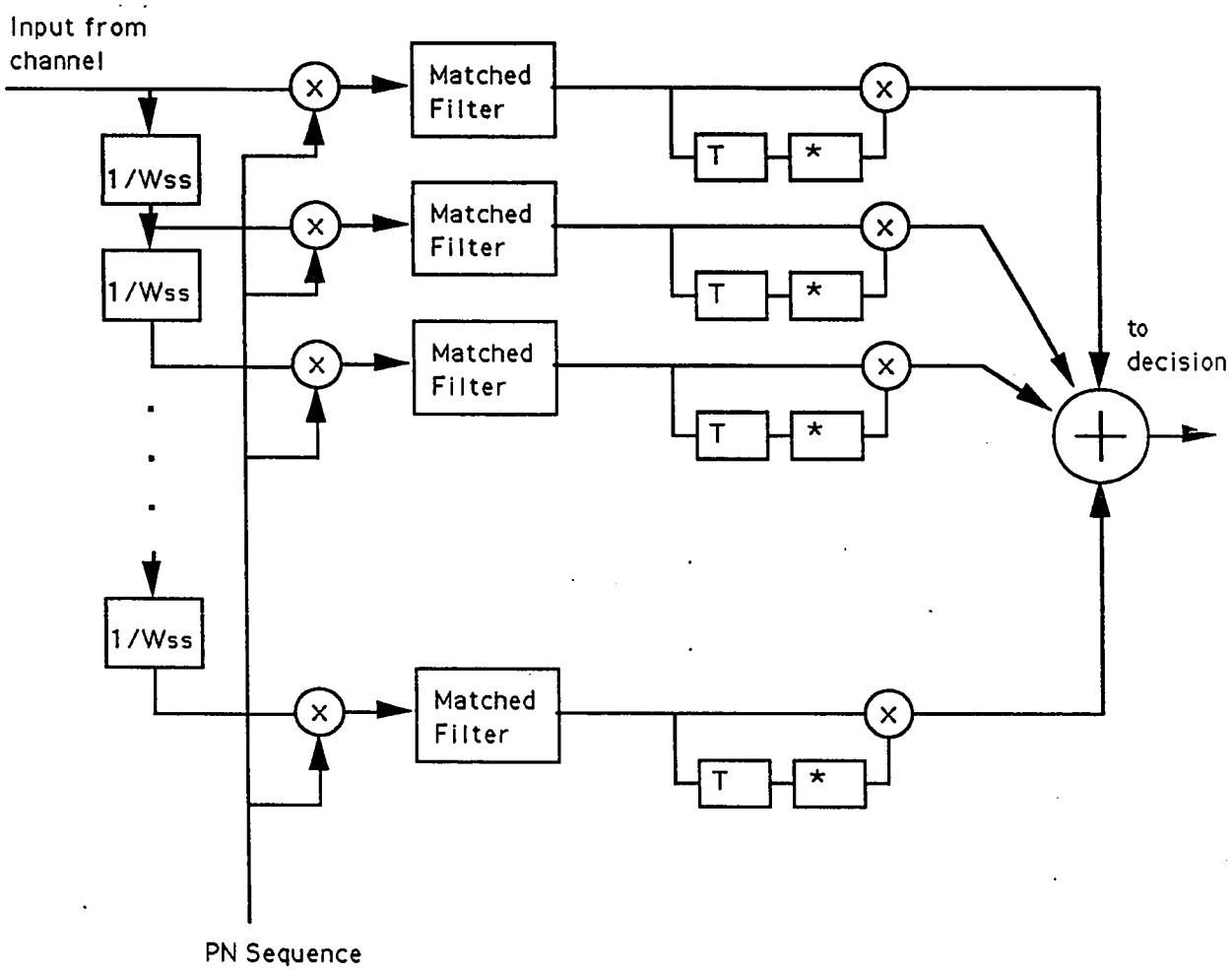

Figure 4.5: Differential RAKE receiver.

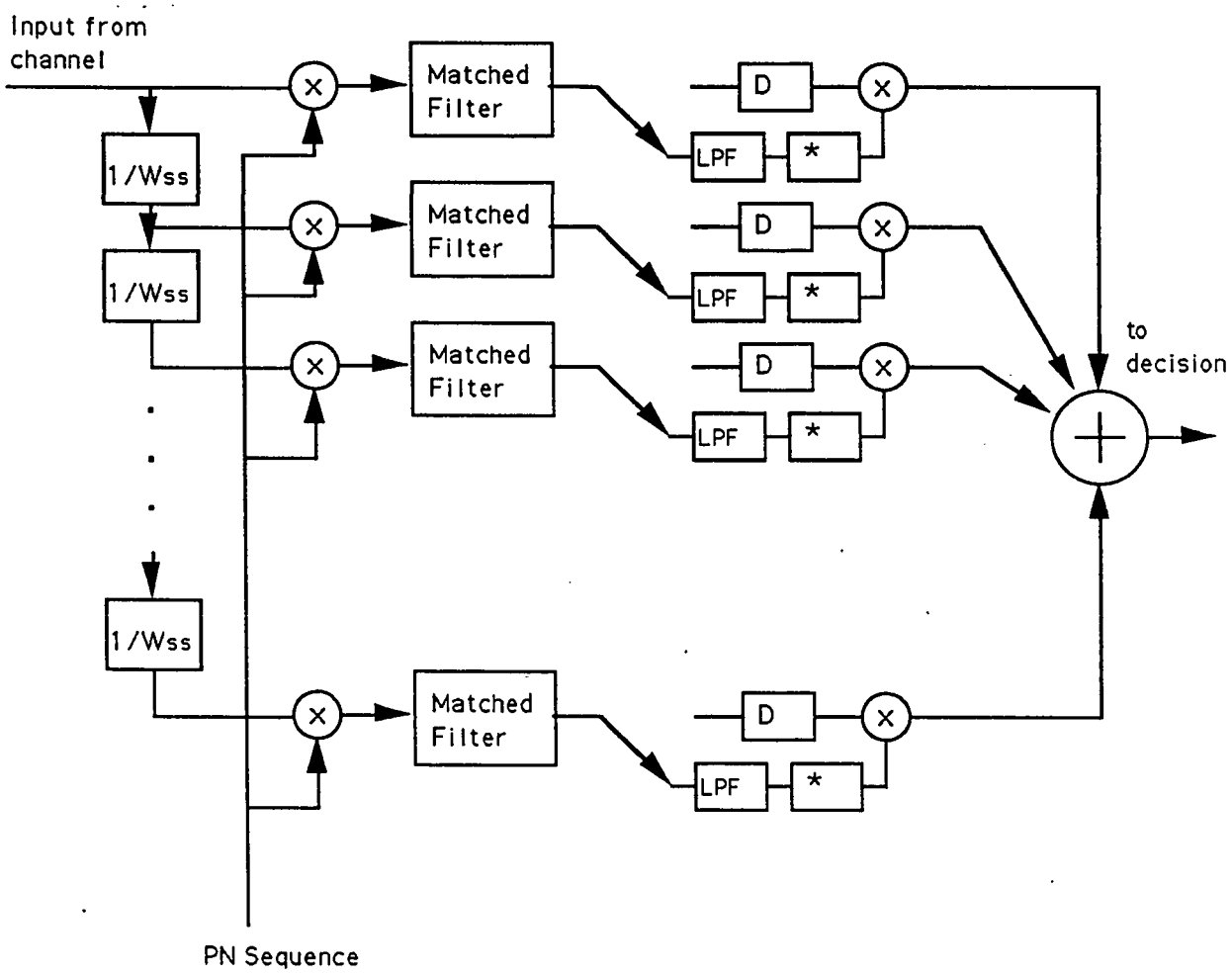

Figure 4.6: Pilot symbol-aided RAKE receiver.

4.2.3 Multisymbol Differential Detection RAKE Receiver

Conventional differential detection observes the incoming signal over two symbols, and makes its decision based on the phase change over these two symbols. Multiple symbol differential detection observes the signal over a longer period and makes a joint decision based on maximum-likelihood sequence estimation. This is further discussed in [12,13].

Figure 4.7 shows the block diagram of an MSDD receiver for a flat fading environment with a detection window of 3. The receiver is divided into two sections. The first section contains the differential detectors. At this point, differential detection is performed on one and two bit intervals. The outputs of these detectors are input to a decision circuit which consists of a hypothesis testing algorithm which is followed by a maximum-likelihood sequence estimator.

For a frequency-selective channel, each tap on the RAKE receiver would contain the differential detectors. The output of these detectors are combined with the output of the appropriate differential detectors on the other RAKE taps. The hypothesis testing is done on the output of these summers. This is shown in Figure 4.8.

4.3 Summary

Diversity combining techniques were described in this chapter. Maximal-gain diversity is the optimum diversity technique for coherent detection in Rayleigh fading. Square-law diversity approximates maximal-gain diversity for non-coherent signalling such as FSK, and equal-gain diversity approximates maximal-gain diversity for differential PSK.

RAKE receivers along with direct-sequence spread spectrum transform frequency-selective Rayleigh fading channels into diversity systems. Structures were given for coherent detection with maximal-ratio diversity, differential detection with equal-gain diversity and multiple symbol differential detection with equal-gain diversity.

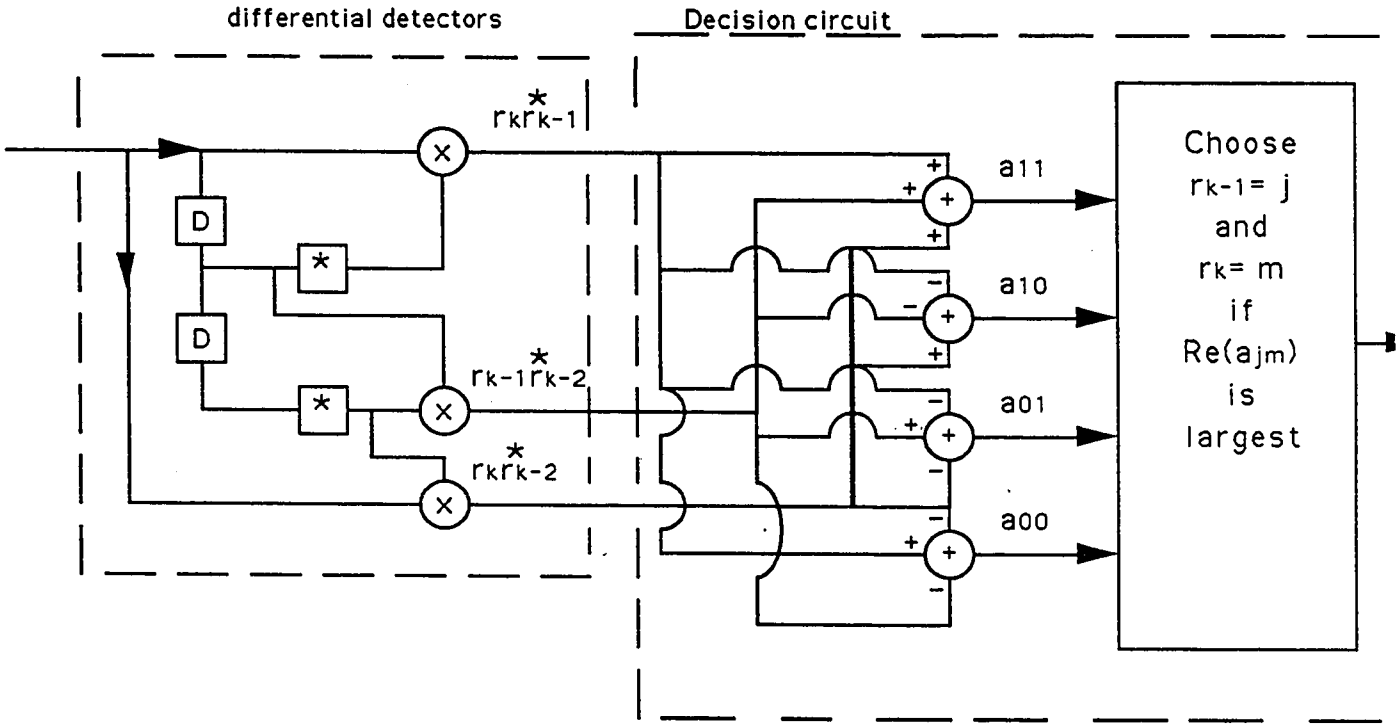

Figure 4.7: Multiple symbol differential detector with detection window of 3.

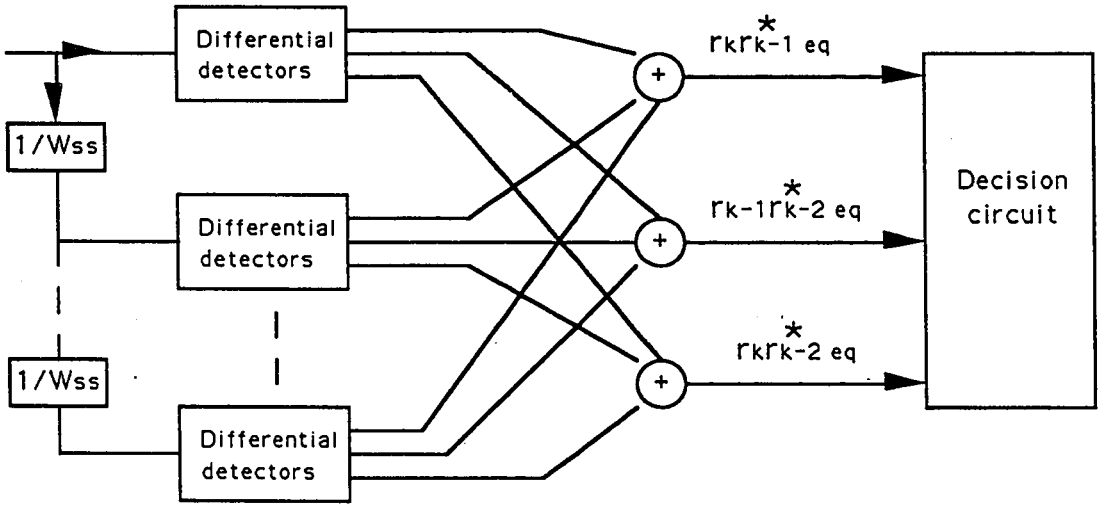

Figure 4.8: MSDD RAKE receiver.

Chapter 5

Simulation Methods and Results

All simulations were performed on LINKSIM, a program developed at the Communications Research Centre (CRC) in Ottawa. The LINKSIM program is capable of simulating a complete communications link at complex baseband. This program was modified and expanded at the University of Ottawa in order to perform the simulation of diversity reception techniques in a frequency-selective Rayleigh fading channel.

5.1 System Modelling

The system to be modelled is as follows:

1) BPSK modulation is used with an information rate of 10 kbps.

2) The spreading sequence is 128 chips long, repeated each information bit. This gives rise to a spread bandwidth of 1.28 MHz.

3) The bandwidth of the fading process is 125 Hz (single-sided), and the fading effects are considered to be constant over the duration of one symbol time.

4) Except for the fading, the channel is assumed to be linear. Consequently, no transmit or receive filtering is needed.

Directly modelling the system as above would require a minimum of 128 samples per information bit. This would give rise to extremely long simulations. Therefore the spread spectrum nature of the system is hidden in the channel model.

The spread spectrum frequency-selective Rayleigh fading channel is modelled with 1 to 5 independent Rayleigh flat fading paths using pre-existing models in LINKSIM. Since there exists some correlation between paths in actual frequency-selective Rayleigh fading channels [24], the results obtained from this model will contain a degree of optimism Using a theoretical RAKE receiver in conjunction with direct sequence spread spectrum, the approximation that the path delays are multiples of the chip time can be made. This is not always true in practice. Receiver taps on either side of the true delay will capture a fraction of the path's power. The path can then be reconstructed at the combiner with some loss. This loss depends on the detection technique used.

By making this assumption, the multipath components need not be combined in the channel program. Each independent Rayleigh path is fed directly to the specific RAKE tap (see Figure 5.1). Since the RAKE receiver realigns all paths before combining them, the delays of each independent path can be ignored.

Since each path is seen as nearly white noise by every other path in a CDMA system, the noise power seen by each receiver tap must be increased by the appropriate factor. If each multipath component is treated as another user's signal, the factor that the noise must be increased by is seen in [8]. This is given by $(1 + \sum_i x_i/B_c)$ where x_i is the average energy per bit energy per noise density ratio of an interfering multipath component, and B_c is the spreading factor of the CDMA system.

In LINKSIM the RAKE receiver is modelled using the pre-existing receiver model. This allows for the use of multitap receivers.

The overall communication link simulated is shown in Figure 5.2. The subprograms developed as a part of this research are shown in italics.

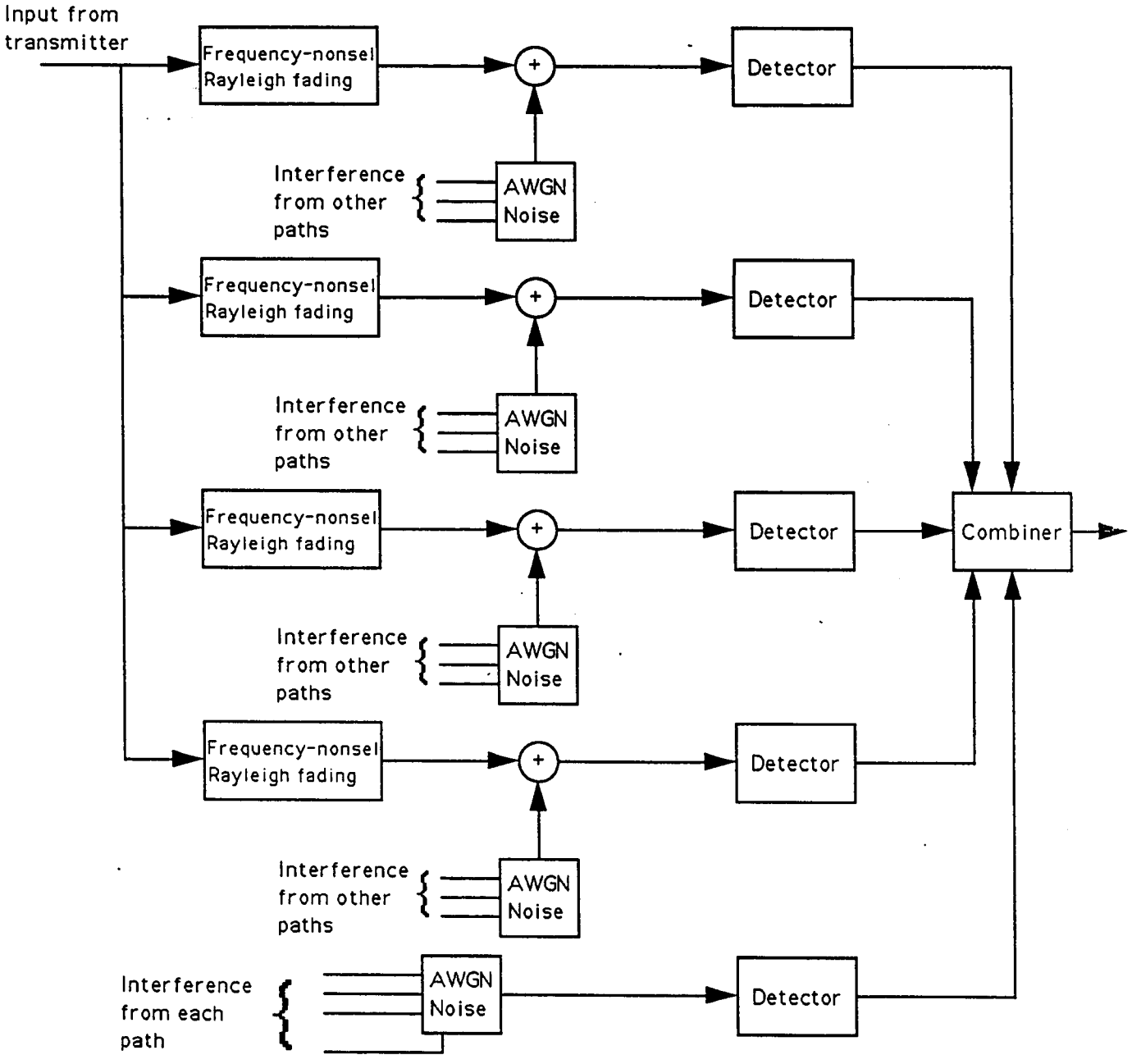

Figure 5.1: Interaction between multipath channel and RAKE receiver programs.

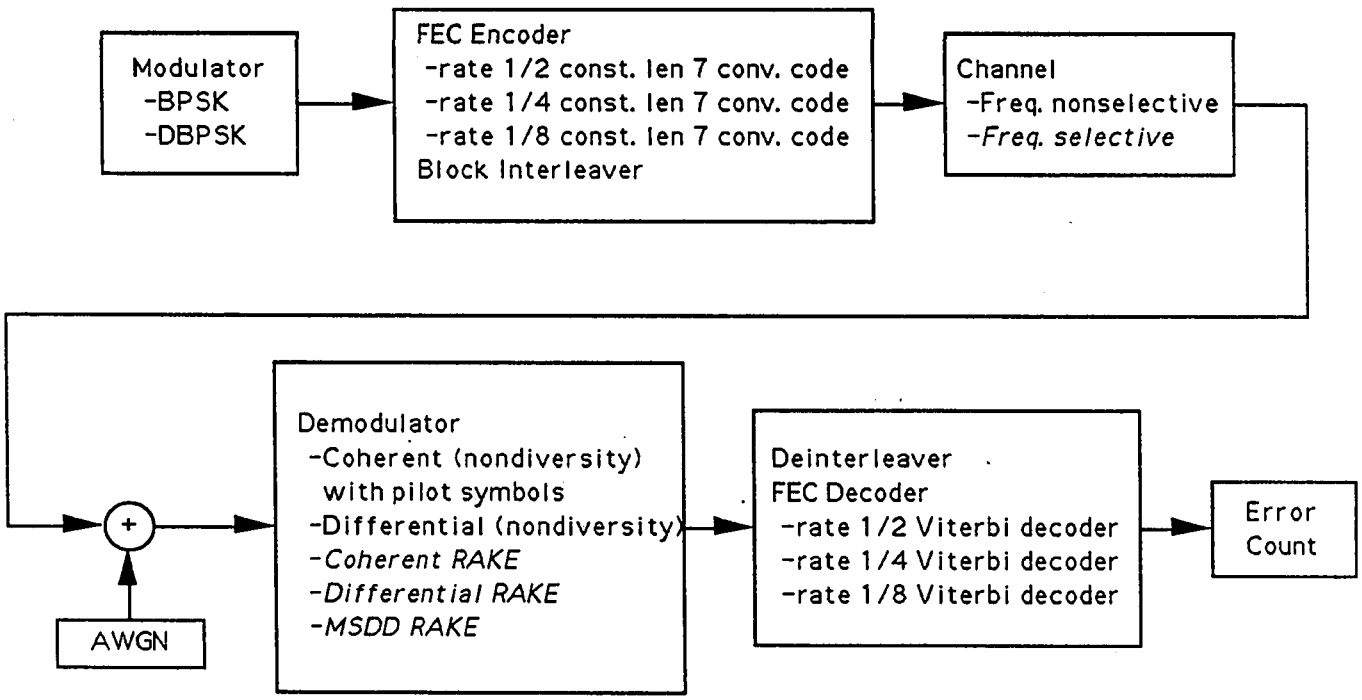

Figure 5.2: Block diagram of LINKSIM implementation.

5.2 System Conditions

The objective of this study is to determine a reliable detection/coding scheme for a CDMA system on a frequency selective Rayleigh channel with RAKE reception. This is considered for channels with a different number of paths as well as perfect and nonideal RAKE receivers.

An ideal RAKE receiver receives all paths of sufficient power and only taps containing a path contributes to the decision. However, in reality, not all paths are received, and noisy taps sometimes contribute to the decision. In these cases, the right choice of detection and coding schemes may suppress the noisy taps.

The simulations performed consider the following Rayleigh fading channels:

(i) 1 Rayleigh path,

(ii) 3 independent Rayleigh fading paths of equal power,

(iii) 5 independent Rayleigh fading paths of equal power,

(iv) 5 independent Rayleigh fading paths of exponentially decreasing power (0dB, -2dB, -4dB, -6dB, -8dB).

The performance of the following schemes are simulated under the channel conditions listed above:

(i) differential detection with 1 tap receiver,

(ii) differential detection with 5 tap receiver with equal gain combining,

(iii) pilot symbol-aided detection with 1 tap receiver,

(iv) pilot symbol-aided detection with 5 tap receiver with maximal ratio combining,

(v) multisymbol differential detection (detection window = 3) with 1 tap receiver,

(vi) multisymbol differential detection with 5 tap receiver with equal gain combining.

For the cases when the channel has more paths than the receiver has taps (eg. 5 paths 1 tap) this is equivalent to an increase in noise only. These simulations are not run since one needs only to shift the bit error rate curve of the 1 path channel with the one tap receiver case. The curves of the one path case are shifted to account for the fraction of received signal energy that is used and must include the increase in noise due to spread spectrum multipath interference. The signal energy that is discarded by the receiver must also be taken account.

In pilot symbol-aided detection, 20% of the power is allocated to the pilot. The pilot is inserted after every four channel symbols.

In addition to these channels and receivers, forward error correction is also considered. The reason for examining the effect of forward error correction is to find powerful combinations of detection and coding strategies, and to find the best tradeoff between coding and receiver complexity. Convolutional codes are chosen because they are powerful and their codecs are commercially available. Their selection does not imply that these codes will provide the optimum results.

Convolutional encoders employ memory and their n outputs depend not only on their k inputs but also on m previous input blocks. These codes have a rate k/n and a constraint length m. For a more detailed description of convolutional codes, the reader is referred to [36].

The coding schemes considered are:

(i) rate 1/2 constraint length 7 convolutional code (r1/2c7),

(ii) rate 1/4 constraint length 7 convolutional code (r1/4c7),

(iii) rate 1/8 constraint length 7 convolutional code (r1/8c7),

The properties of these codes in an AWGN channel [36] are given in Table 5.1.

It should be noted that these three codes provide the same coding gain in AWGN channels and it is for this reason that codes of different constraint lengths are not considered.

In all cases Viterbi decoding [36] is used. All codes employ soft decisions with the

code	r1/2c7	r1/4c7	r1/8c7
rate	1/2	1/4	1/8
constraint length	7	7	7
free distance	10	20	40
coding gain (dB)	7	7	7

Table 5.1: Code properties in AWGN.

exception of when MSDD is used. Since the existing MSDD software requires a decision to be made in the detection process, soft decision cannot be employed for this technique. Note that it is possible to modify the MSDD software such that it employs a Viterbi decoder. Then it would be possible to use MSDD with soft decision decoding [13]. However, this results in a large increase in complexity.

Interleaving is used in all cases. A 40 ms (400 information bits) interleaver is used. The interleaving is performed on a coded symbol level.

All simulations include AWGN as the only source of interference. The bit error rate objective is 10^{-3}, as would be required for digital speech.

The parameter E_b/N_o refers to the ratio between the average received energy per information bit to the single sided noise spectral density of the channel. In the case of a single path channel, E_b is the signal energy of that path. In the case of a multiple path channel, E_b refers to the sum of the average energies of all the paths.

5.3 Simulation Results

The results discussed in this section are grouped together according to channel and receiver conditions with a separate graph for each detection type. For all performance curves, a minimum of 1000 bit errors were tabulated for each point. Curves are given for

(i) uncoded,

(ii) rate 1/2 coded convolutional code with constraint length 7 (r1/2c7),

(iii) rate 1/4 coded convolutional code with constraint length 7 (r1/4c7),

(iv) rate 1/8 coded convolutional code with constraint length 7 (r1/8c7),

All codes employ a 40 ms (400 bit) block interleaver/deinterleaver.

5.3.1 AWGN Channel

Figure 5.3 demonstrates the performance of the different coding schemes for coherent detection in AWGN. The three convolutional codes have the same asymptotic coding gain, but at a bit error rate of 10^{-3}, rate 1/8 convolutional code outperforms the other codes.

Figure 5.4 demonstrates the performance of the codes in AWGN when differential detection is used. No interleaving is included in this simulation. Note that the performance of the codes is much worse than for coherent detection (Figure 5.3). The relative performance of the codes are practically reversed as in Figure 5.3. Bit errors in DBPSK tend to occur in pairs. These small error bursts are enough to seriously degrade the performance of the convolutional codes, which are random error correcting codes. The lower rate codes have smaller symbol energies, therefore these double errors occur with a greater frequency than in the higher rate codes, and thus their performance is worse. This figure demonstrates the need for adequate interleaving in order to randomize symbol errors.

Figure 5.5 shows the decoding of DBPSK in an AWGN channel with interleaving. The performance of each coded curve improves slightly, but their relative performance remains unchanged. In other words, even with the elimination of the double errors common to DBPSK, the lower rate codes still perform worse than the higher rate codes. This result suggests that differential detection causes some loss in performance in lower rate codes. Although coherent detection outperforms differential detection by 0.8dB at higher values of E_b/N_o in AWGN channels, at lower values of E_b/N_o, the gain can be as much as 4dB [10]. When low rate codes are used, the energy per code symbol, E_{cs}, becomes quite small. For the bit energies considered, the lower rate codes produce values of E_{cs}/N_o which are quite low. Therefore, the lower the rate of the code, the larger the difference in performance

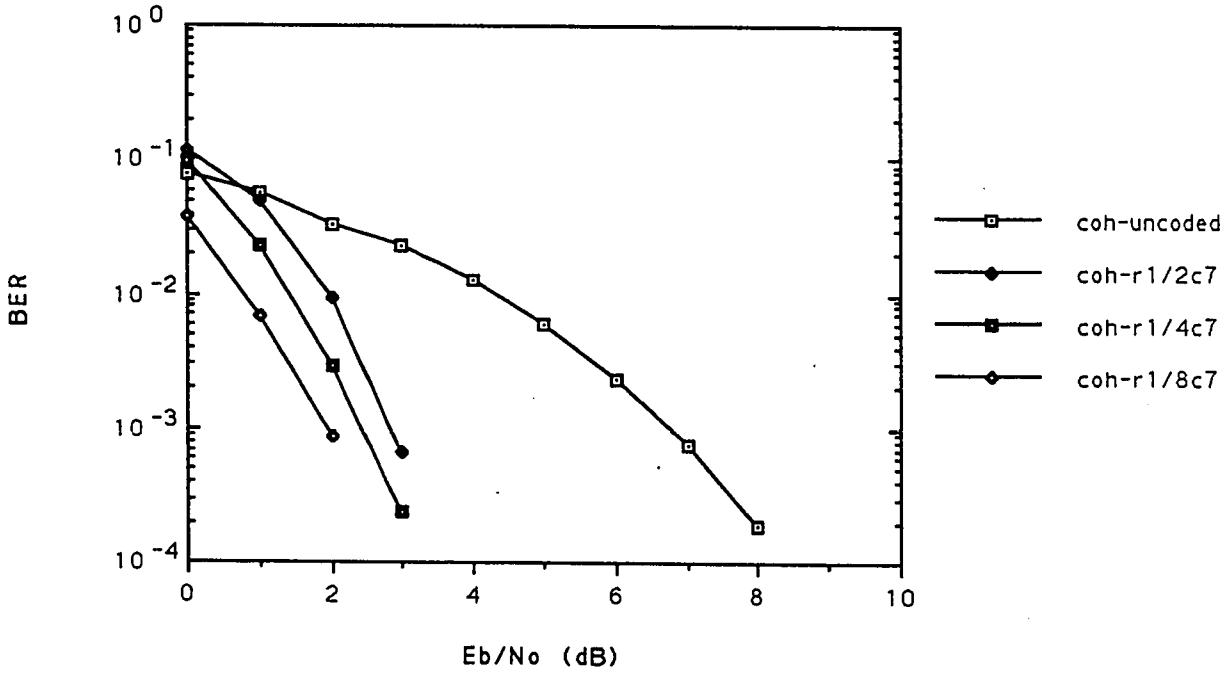

Figure 5.3: Coherent detection in an AWGN channel.

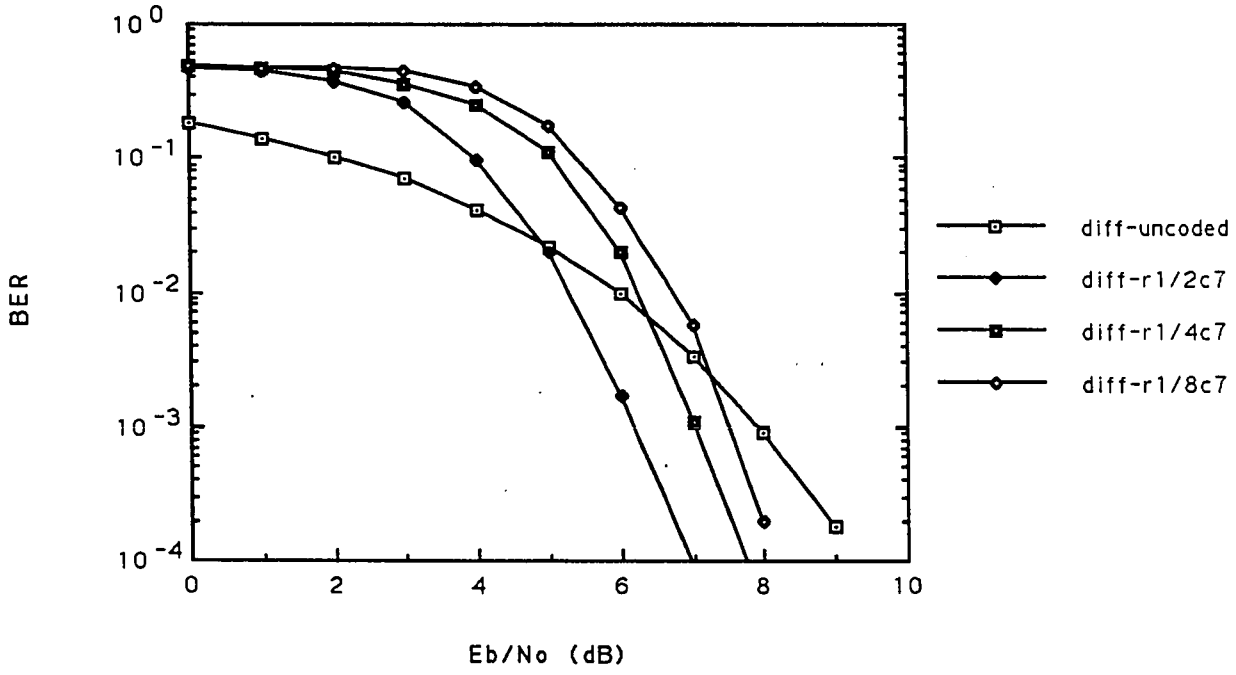

Figure 5.4: Differential detection in an AWGN channel - No interleaving.

between coherent and differential detection.

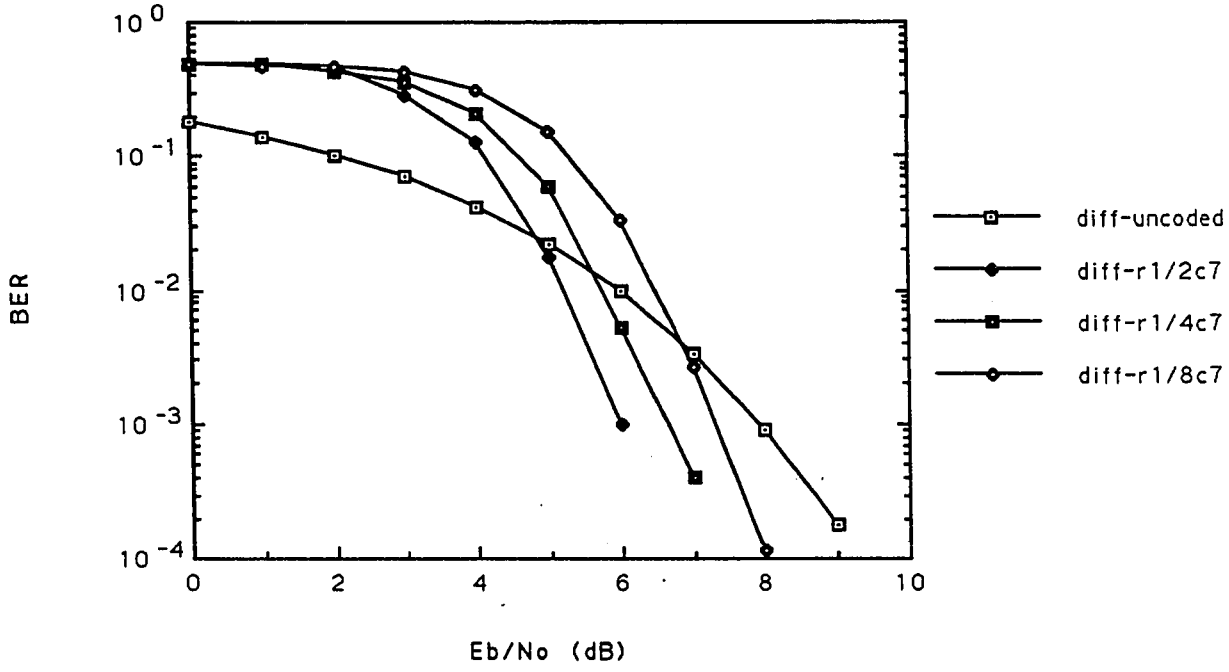

Figure 5.5: Differential detection in an AWGN channel with interleaving.

5.3.2 Single Path (Frequency-Nonselective) Rayleigh Channel

Figure 5.6 demonstrates the performance of differential detection for a single path channel by a single tap receiver. The uncoded case matches the theoretical curve obtained from [10]. When coding is used, it is difficult to determine the best

scheme as most of the curves reach the target bit error rate of 10^{-3} within a 1dB range. However, the rate 1/8 convolutional code appears to provide a small gain over the other codes.

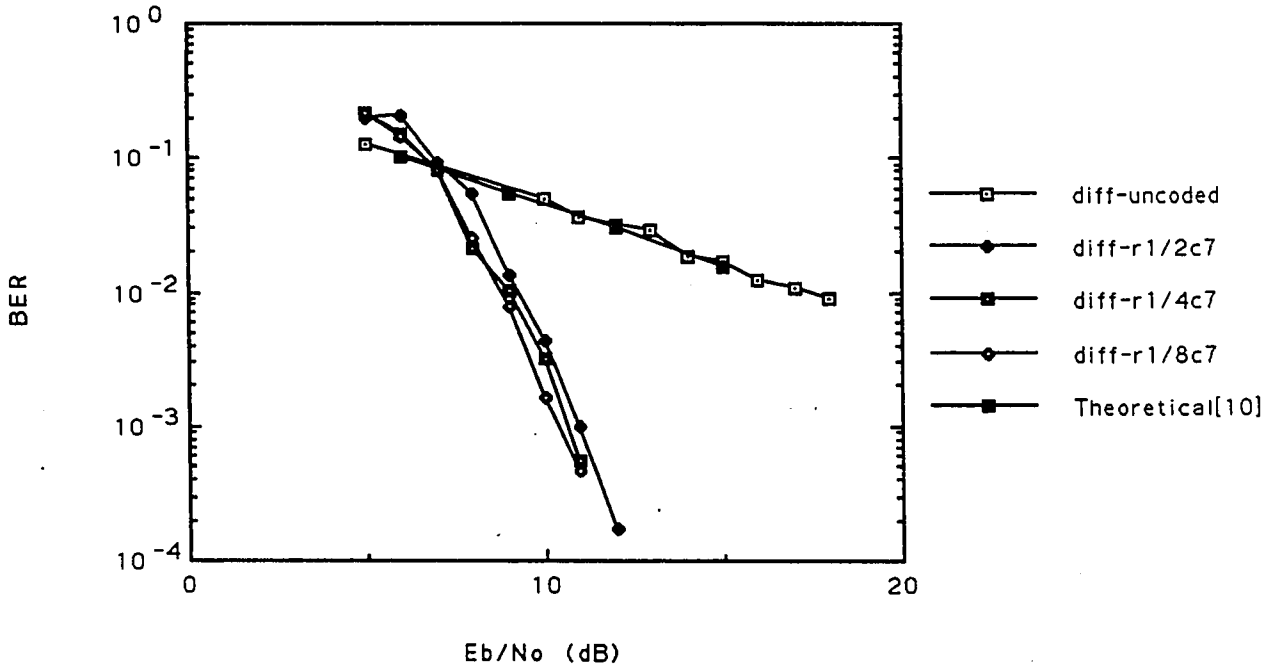

Figure 5.6: Differential detection of spread spectrum in frequency-nonselective Rayleigh fading.

The effect of pilot symbol-aided detection on a single path channel received by a single tap receiver is shown in Figure 5.7. The uncoded curve seen here exhibits the same behaviour as the uncoded curve seen in Figure 5.6. However, pilot symbol-aided detection with a rate 1/8 convolutional code provides a better performance compared to any coded case in Figure 5.6.

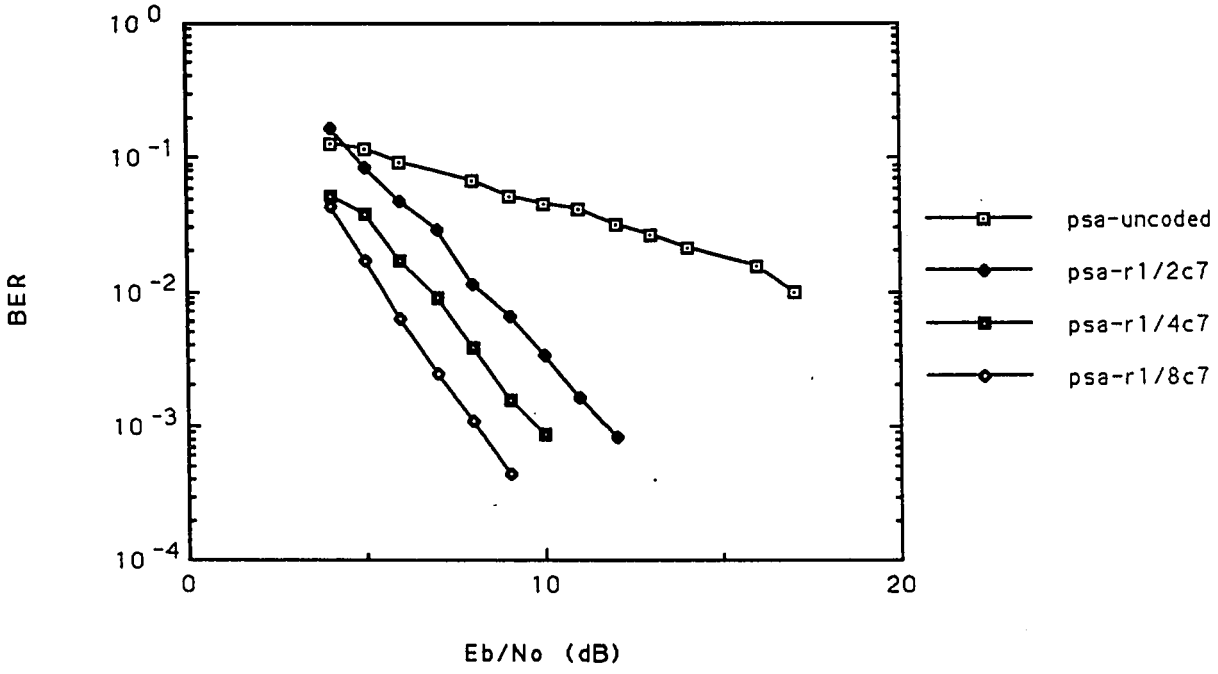

Figure 5.7: Pilot symbol-aided detection of spread spectrum in frequency-nonselective Rayleigh fading.

Figure 5.8 shows the use of a conventional spread spectrum MSDD receiver for a single path channel. The slope of the coded curves are less steep than in Figures 5.6 and 5.7 since the MSDD algorithm used does not allow for the exploitation of soft decisions by the decoder. From this figure, it can be seen that the rate 1/8 convolutional code provides a slight gain over the other coding schemes at a BER of 10^{-3}.

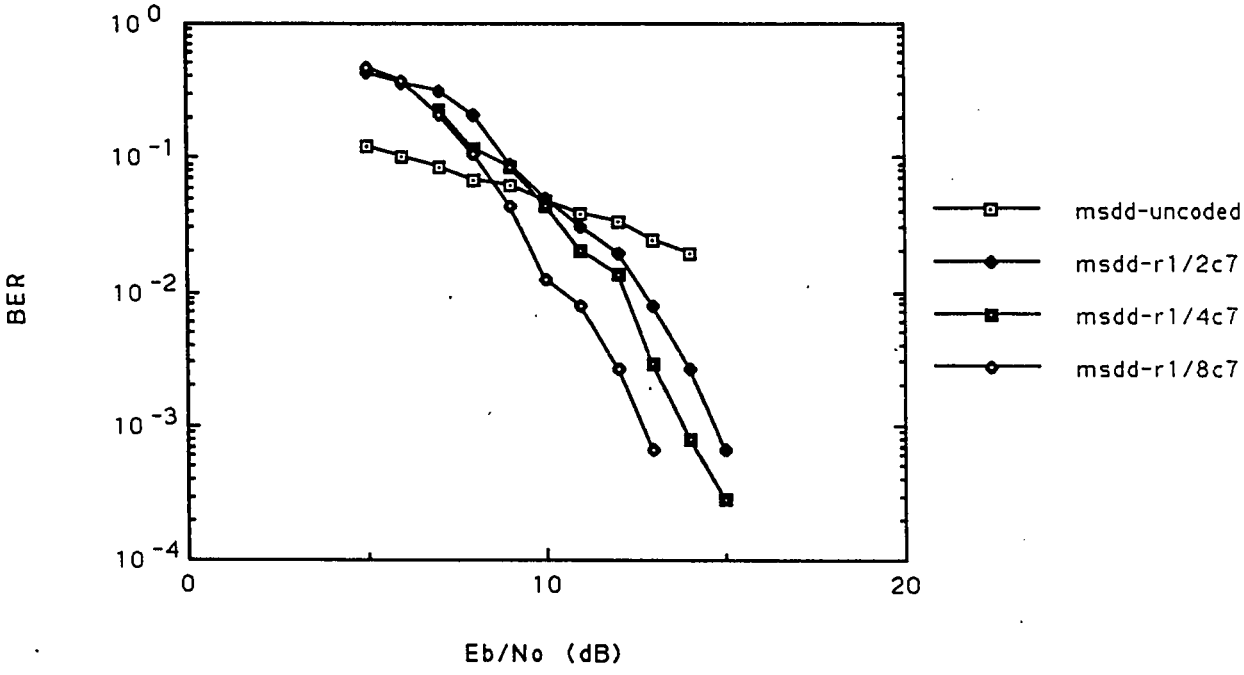

Figure 5.8: Multiple symbol differential detection of spread spectrum in frequency-nonselective Rayleigh fading.

To allow for a direct comparison, Figure 5.9 provides the performance curves for all three detection schemes, uncoded and optimally coded, for the above system

conditions. When no coding is used, all three detection schemes produce curves which are almost identical for the values of E_b/N_o shown. At higher signal energies, it is possible to see that uncoded MSDD slightly outperforms uncoded differential detection. In theory, MSDD should always outperform conventional differential detection in a frequency-nonselective fading environment [12,13].

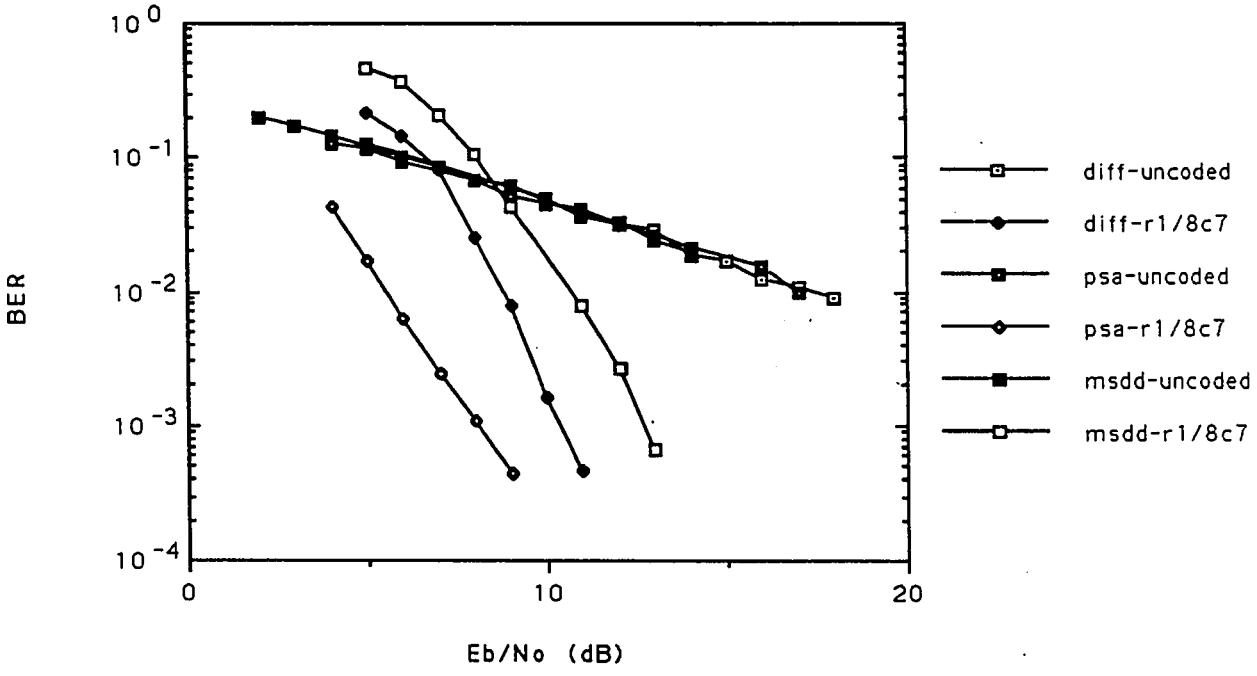

Figure 5.9: Comparison of detection strategies for spread spectrum signals in frequency-nonselective Rayleigh fading.

When the signals are coded, pilot symbol-aided coherent detection with a rate 1/8 constraint length 7 convolutional code provides a BER of 10^{-3} for an E_b/N_o of about 8.3dB. Differential detection, employing the same code, provides this BER

when E_b/N_o is approximately 10.5dB. This indicates that at low values of E_b/N_o, uncoded pilot symbol-aided detection outperforms differential detection. MSDD with rate 1/8 convolutional code with hard decisions requires an E_b/N_o of about 12.5dB in order to provide the target BER.

5.3.3 Single Path Channel - 5 Tap RAKE

In Figures 5.10-5.13, a single path channel is received by a 5 tap RAKE. There are four taps which contain only noise, and it is interesting to see which detection scheme best suppresses the noisy taps.

In Figure 5.10, differential detection with equal gain combining is used. The curves are similar to those in Figure 16, but an increase in noise is evident. The rate 1/8 convolutional code provides the largest coding gain at a BER of 10^{-3}. This BER is obtained when E_b/N_o is about 13.5dB. This translates into a loss of about 3dB from Figure 5.6.

Figure 5.11 demonstrates the use of pilot symbol-aided detection with maximal gain ratio combining for a single path channel with a 5 tap RAKE. The rate 1/8 convolutional code provides the best results in this case. The bit error rate of 10^{-3} is obtained when E_b/N_o is about 10dB. Comparing Figure 5.11 with Figure 5.7, a loss of 1.7dB is obtained when the four noisy taps are present. This clearly demonstrates that pilot symbol detection is much better than differential detection at suppressing noisy taps.

MSDD is seen in Figure 5.12. The rate 1/8 constraint length 7 convolutional code reaches the target bit error rate when E_b/N_o is about 15.9dB. When this result is compared to the result of Figure 5.8, a loss of about 3.4dB occurs when the four noisy taps are present.

The comparison of the different detection types is made in Figure 5.13. It can be seen that uncoded pilot symbol-aided detection performs slightly better than uncoded differential detection and uncoded MSDD. Rate 1/8 convolutionally coded pilot symbol-aided detection is the best detection scheme in this case. About a 4dB advantage is obtained over coded differential detection. In pilot symbol-aided

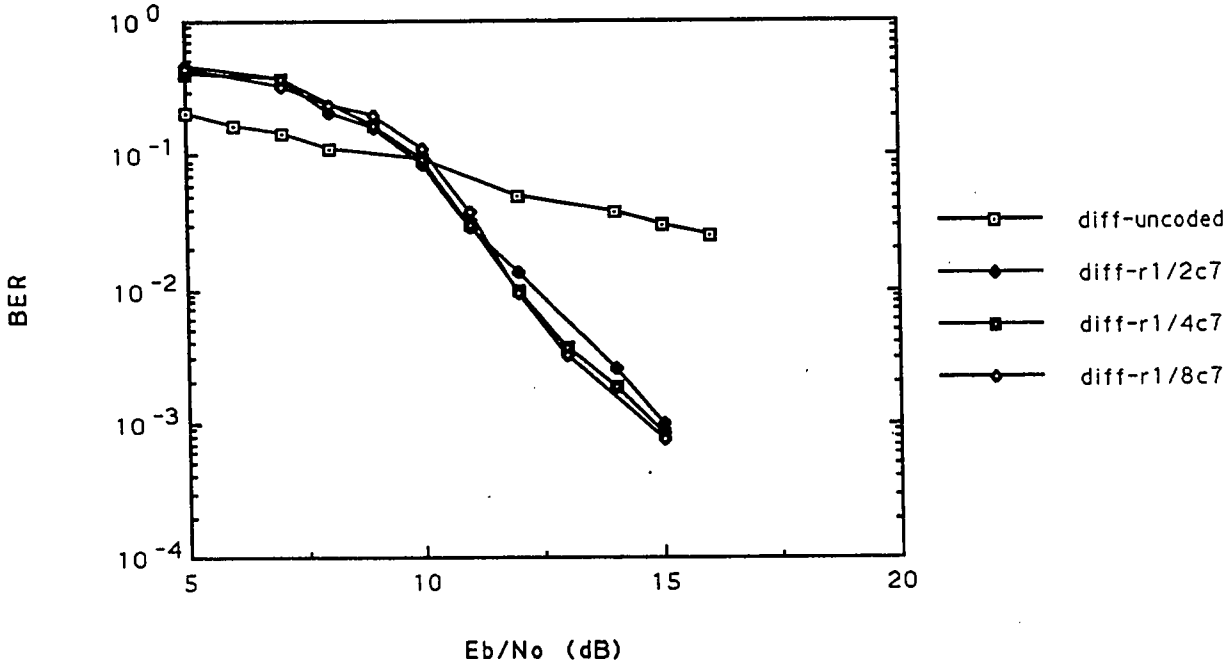

Figure 5.10: 1 path channel - 5 tap differential RAKE receiver.

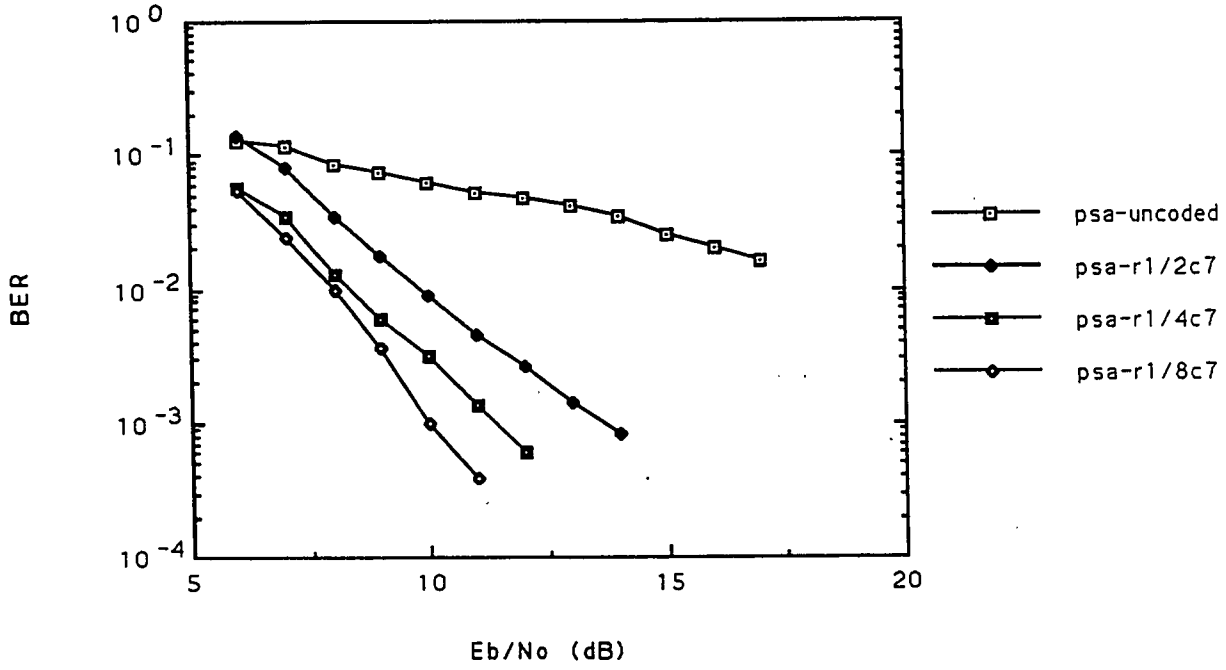

Figure 5.11: 1 path channel - 5 tap pilot symbol-aided RAKE receiver.

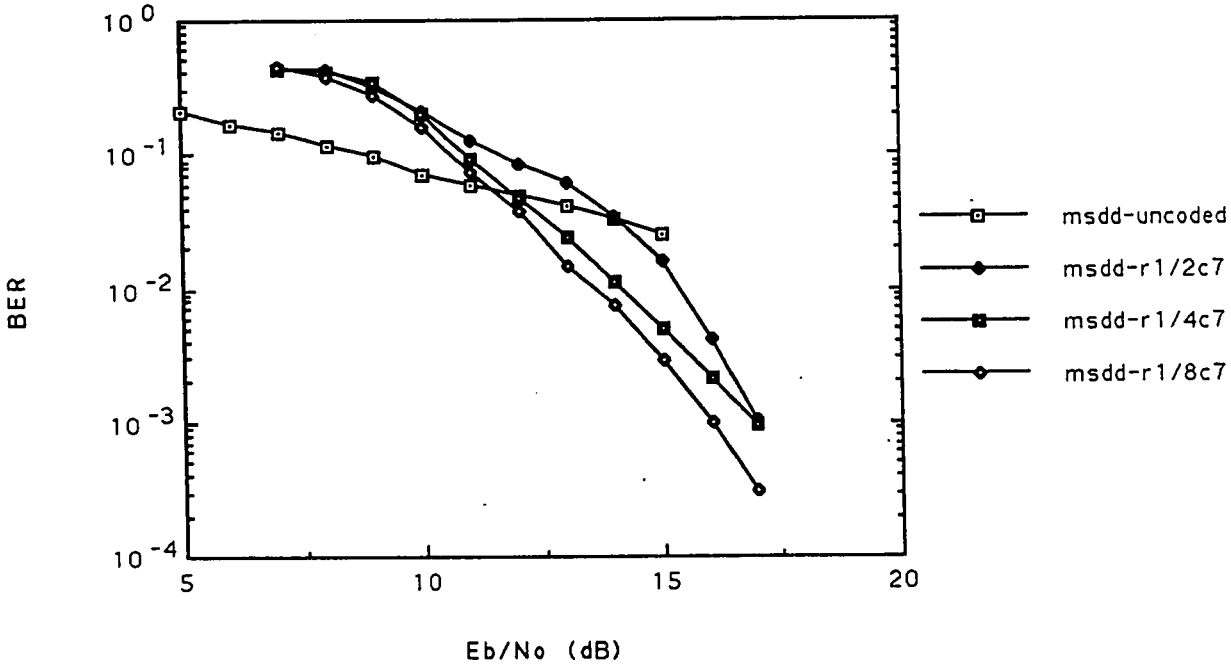

Figure 5.12: 1 path channel - 5 tap MSDD RAKE receiver.

detection, the output of the channel estimator is used to weight the information on each tap for maximal gain ratio combining. A noise signal would be greatly attenuated through the narrowband channel estimation filter. The output of this filter is used to weight the contents of the tap. Therefore noisy taps contribute little to the final decision.

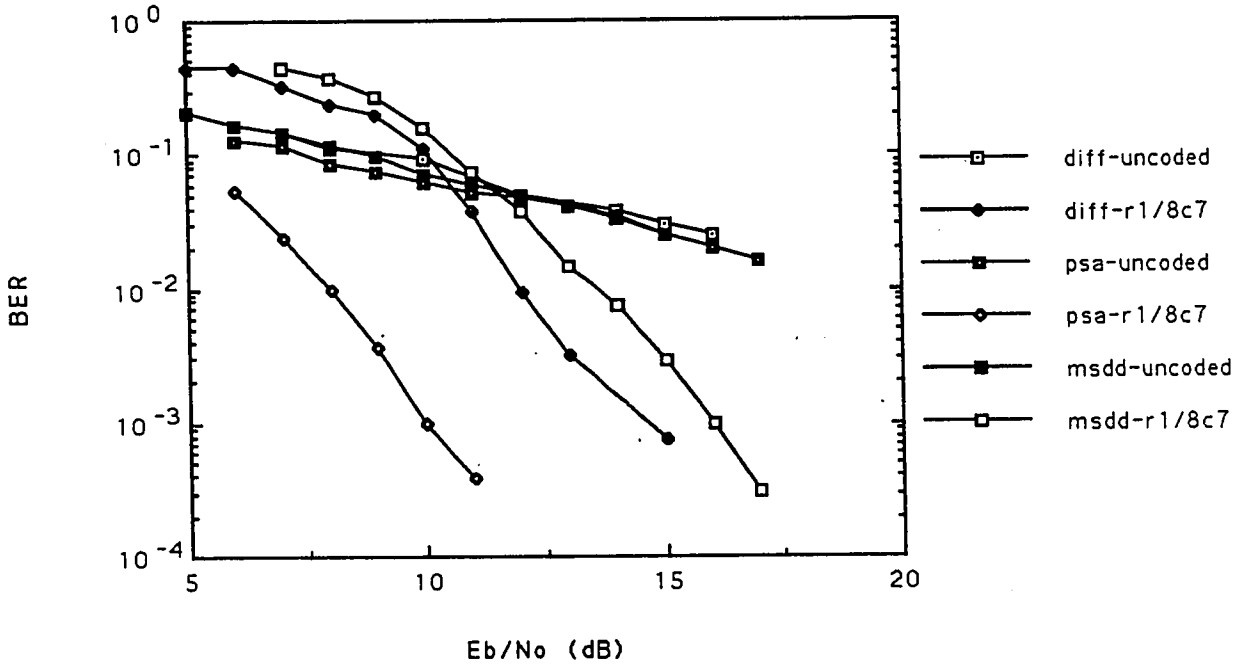

Figure 5.13: Comparison of different detection strategies for 1 path channel - 5 tap RAKE receiver.

5.3.4 3 Path Channel - 5 Tap RAKE

Figures 5.14 to 5.17 demonstrate the performance of a 3 path frequency-selective Rayleigh fading channel received by a 5 tap RAKE. This demonstrates the effect of combining independent paths while noisy taps are present.

Figure 5.14 shows the use of differential detection under this condition. The best coding scheme is the rate 1/2 constraint length 7 convolutional code. It provides a coding gain of about 1dB over the rate 1/4 convolutional code. The target bit error rate is obtained when E_b/N_o is about 10.3dB. In the frequency-nonselective case (Fig. 5.6), the target BER was obtained for an E_b/N_o of 10.5dB with the use of rate 1/8 convolutional code. Using a conventional spread spectrum receiver to receive this 3 path channel, only 1/3 of the overall received signal energy is used, and the remaining 2/3 is converted to noise energy. In section 5.1, the increase in noise due to multipath interference is given as $(1 + \sum_i x_i/B_c)$, where x_i is to interfering multipath signal energy per bit to noise density ratio. Thus the required E_b/N_o for a bit error rate of 10^{-3} for a conventional spread spectrum receiver can be obtained from the following equation:

$$(E_b/N_o)_{ns} = \frac{\frac{1}{3}(E_b/N_o)}{1 + (\frac{2}{3})(E_b/N_o)(\frac{1}{B_c})} \tag{5.1}$$

where $(E_b/N_o)_{ns}$ is the energy to noise density required for a bit error rate of 10^{-3} in the frequency-nonselective case (10.5dB). Performing this calculation determines that a conventional spread spectrum receiver requires that E_b/N_o be equal to 16.1dB. Therefore, about 5.8dB is gained by using a 5 tap RAKE receiver with rate 1/2 convolutional coding over conventional spread spectrum reception with rate 1/8 convolutional coding.

Figure 5.15 presents pilot symbol-aided detection under these system conditions. Rate 1/8 convolutional code is the best coding scheme. The target BER is obtained when E_b/N_o is about 8dB. Using the results of Figure 5.7, a single tap receiver employing rate 1/8 convolutional code would provide the bit error rate of 10^{-3} when E_b/N_o is about 13.9dB. The RAKE receiver provides a gain of about 5.9dB.

The performance of MSDD is shown in Figure 5.16. The best coding scheme is

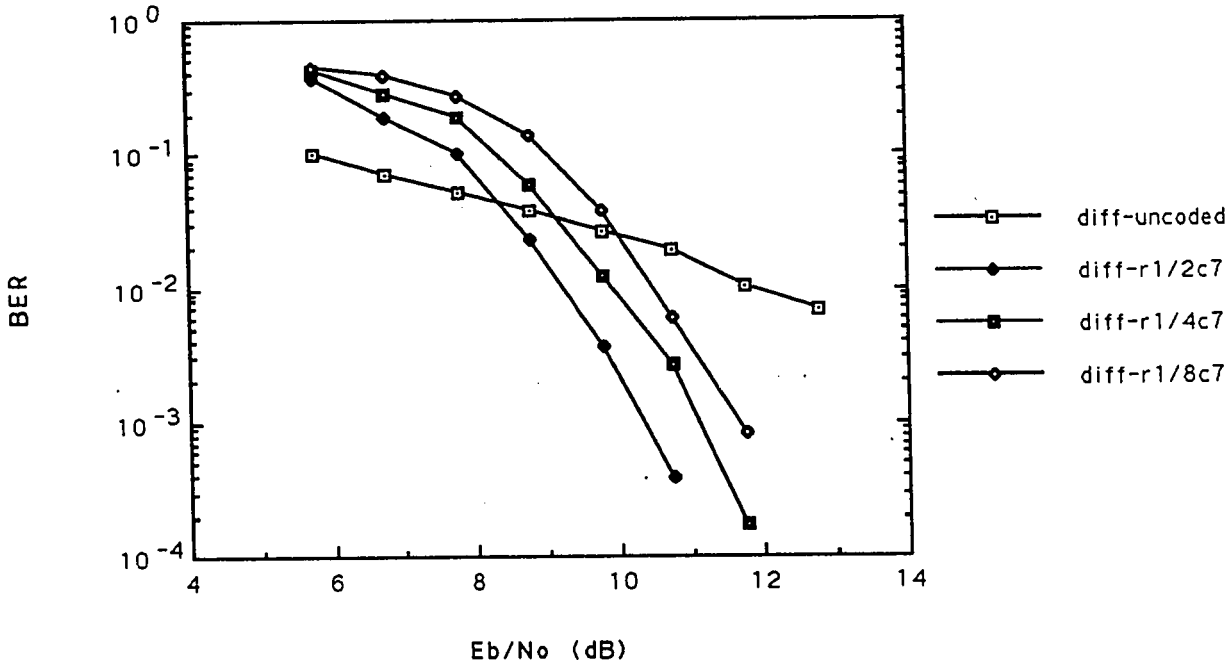

Figure 5.14: 3 path channel - 5 tap differential RAKE receiver.

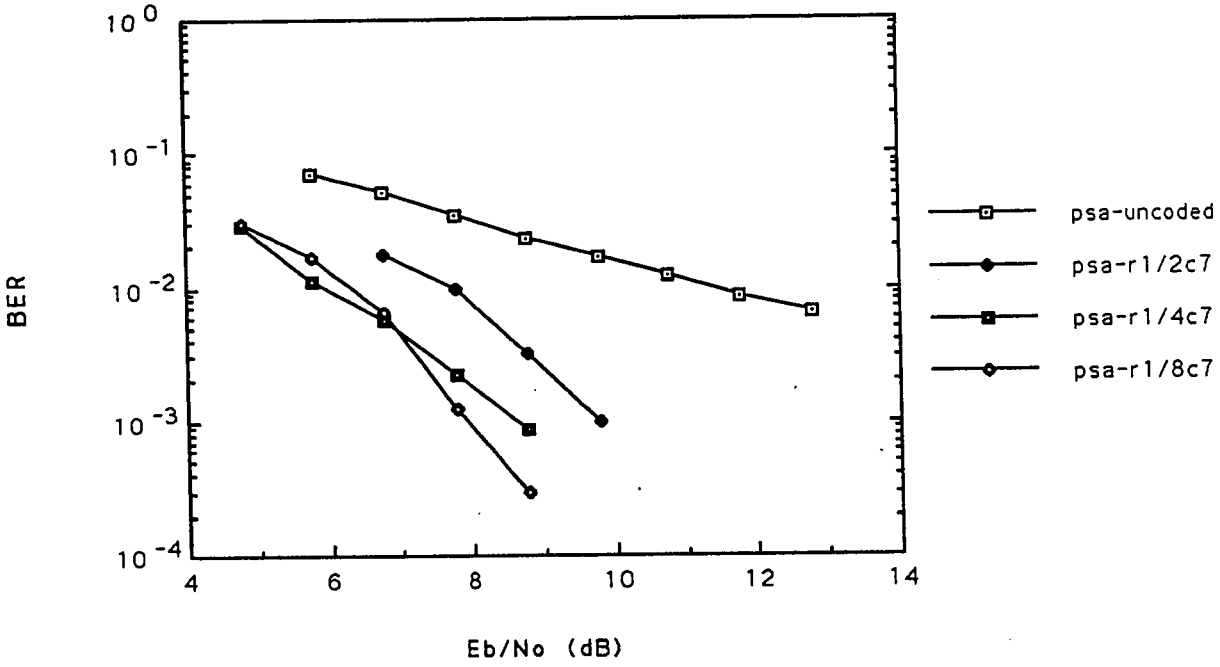

Figure 5.15: 3 path channel - 5 tap pilot symbol-aided RAKE receiver.

the rate 1/2 constraint length 7 convolutional code. The bit error rate of 10^{-3} is obtained when E_b/N_o is about 12.3dB. From the flat fading results of Figure 5.8, a single tap receiver, employing rate 1/8 convolutional code, would require a received signal energy to noise density ratio of 19.2dB. A gain of 6.9dB is obtained by employing a 5 tap RAKE receiver.

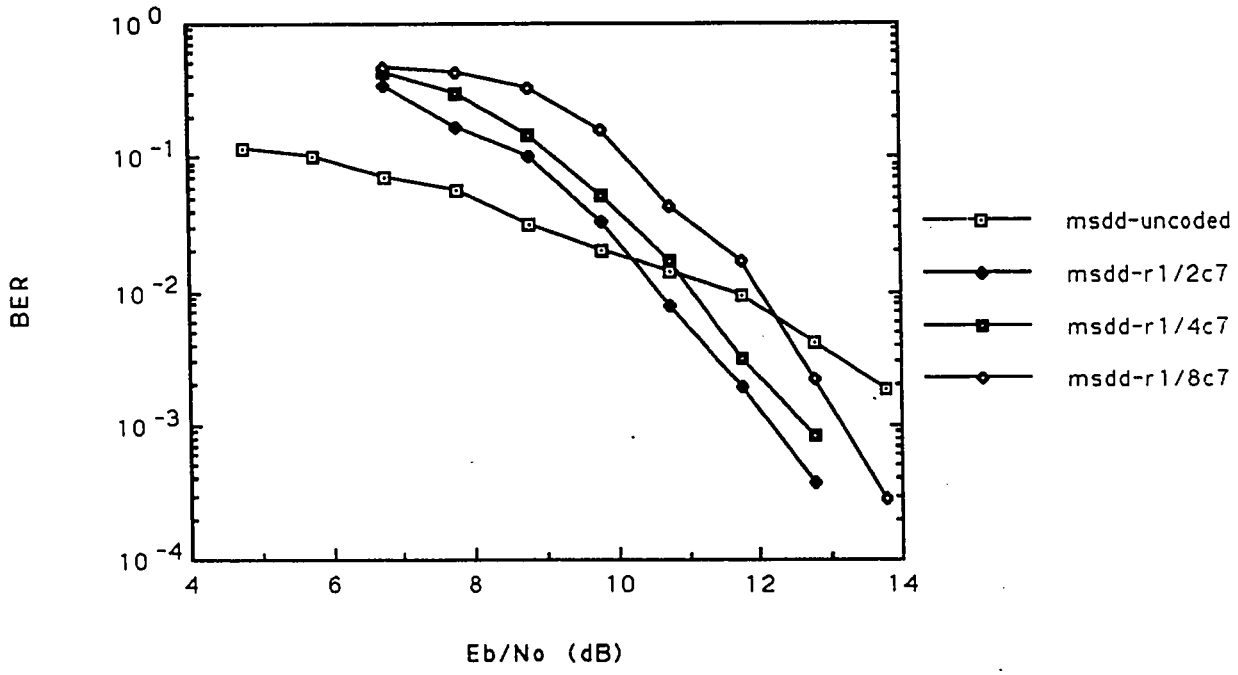

Figure 5.16: 3 path channel - 5 tap MSDD RAKE receiver.

Figure 5.17 compares the three detection schemes for the three path channel received by a 5 tap RAKE. Uncoded pilot symbol-aided detection performs slightly better than uncoded differential detection and uncoded MSDD. Uncoded MSDD slightly outperforms uncoded differential detection. When coding is used, pilot

symbol-aided coherent detection with a rate 1/8 convolutional code provides about a 2.3dB advantage over rate 1/2 convolutionally coded differential detection. Rate 1/2 convolutionally coded MSDD, which employs hard decision decoding, does not perform as well.

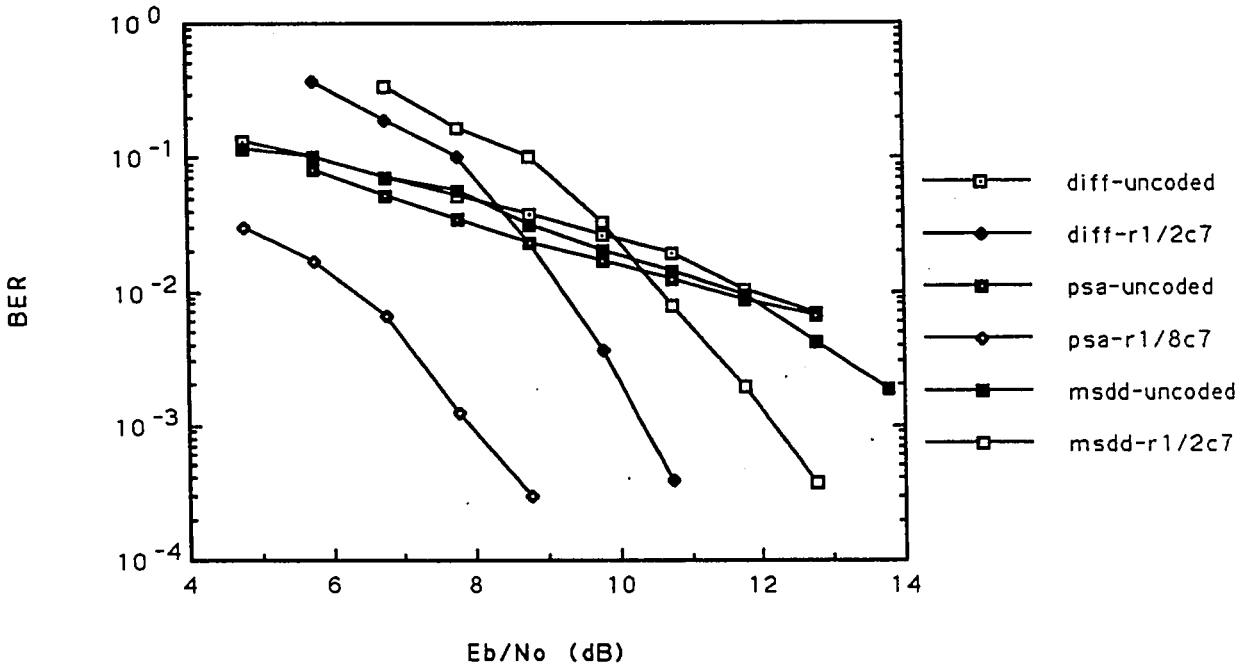

Figure 5.17: Comparison of different detection strategies for 3 path channel - 5 tap RAKE receiver.

5.3.5 5 Path Frequency Selective Channel - 5 Tap RAKE

Figures 5.18 to 5.21 demonstrate the reception of 5 independent Rayleigh faded paths by a 5 tap RAKE. These figures demonstrate perfect RAKE reception as no noisy taps are present.

Differential detection is seen in Figure 5.18. Turin considers the use of differential detection for RAKE reception in [27] and he simulates perfect RAKE reception without the use of coding. In his simulations, he considers a spreading factor of 127 chips/bit which is quite close to the spread factor of 128 used in these simulations. The results obtained from LINKSIM are compared to those given by Turin and they are virtually identical.

When coding is used, the rate 1/2 constraint length 7 code provides the best results. By employing this code, the bit error rate of 10^{-3} is obtained when E_b/N_o is about 9.5dB. The use of a conventional spread spectrum receiver, which uses only 1/5 of the overall signal energy, requires that the received single path have an $E_b/(N_o + I)$ of 10.5dB (from Figure 16), where I is the spread spectrum multipath interference, and rate 1/8 convolutional coding is used. Using the same method of calculation as in the 3 path - 5 tap case, the required E_b/N_o can be found to be 19dB for a conventional spread spectrum receiver. The use of a RAKE receiver provides a gain of about 9.5dB.

Figure 5.19 depicts the use of pilot symbol-aided coherent detection for this channel condition. The best coding scheme is the rate 1/8 constraint length 7 convolutional code. The target bit error rate is obtained when E_b/N_o is about 7.5dB. A conventional spread spectrum receiver would require an E_b/N_o of 16.3dB (for rate 1/8 coding) under this channel condition. A gain of about 8.8dB can be obtained by employing a RAKE receiver.

Figure 5.20 demonstrates the use of MSDD for these system conditions. The uncoded curve exhibits the same behaviour as the uncoded differential curve of Figure 5.18. Due to the use of hard decision decoding, the performance of coded MSDD is worse than the performance of coded differential and pilot symbol-aided detection strategies. The target bit error rate is obtained when E_b/N_o is about 11.2dB. From the single path results, it can be shown that a conventional spread

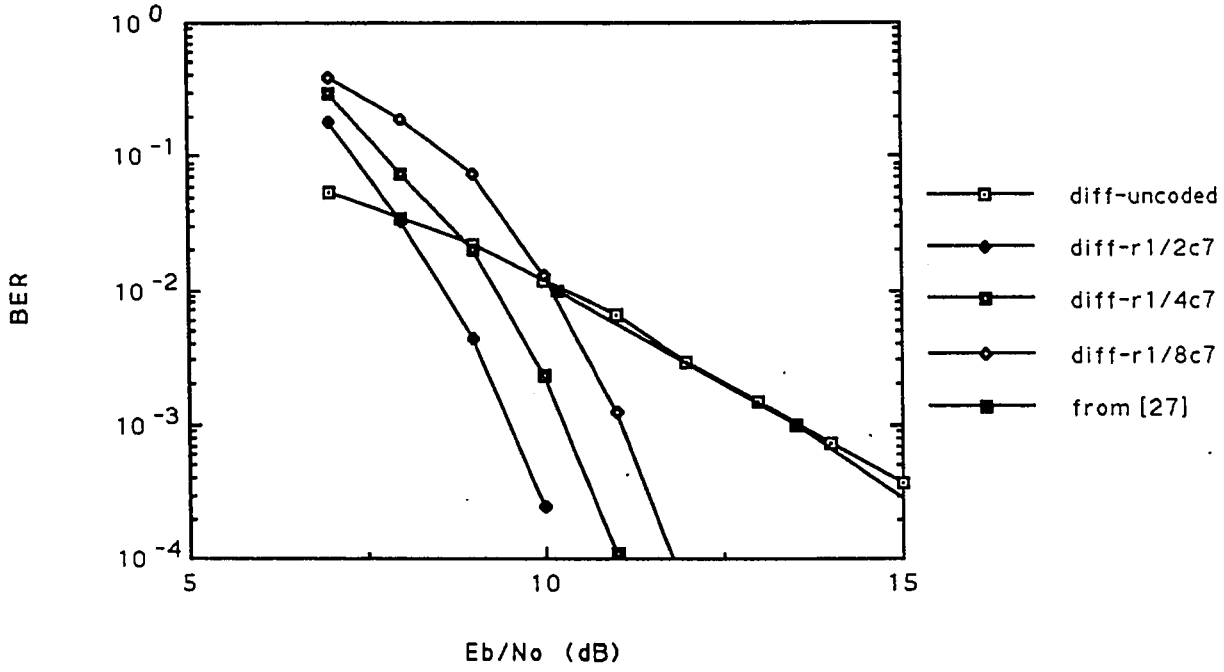

Figure 5.18: 5 path channel - 5 tap differential RAKE receiver.

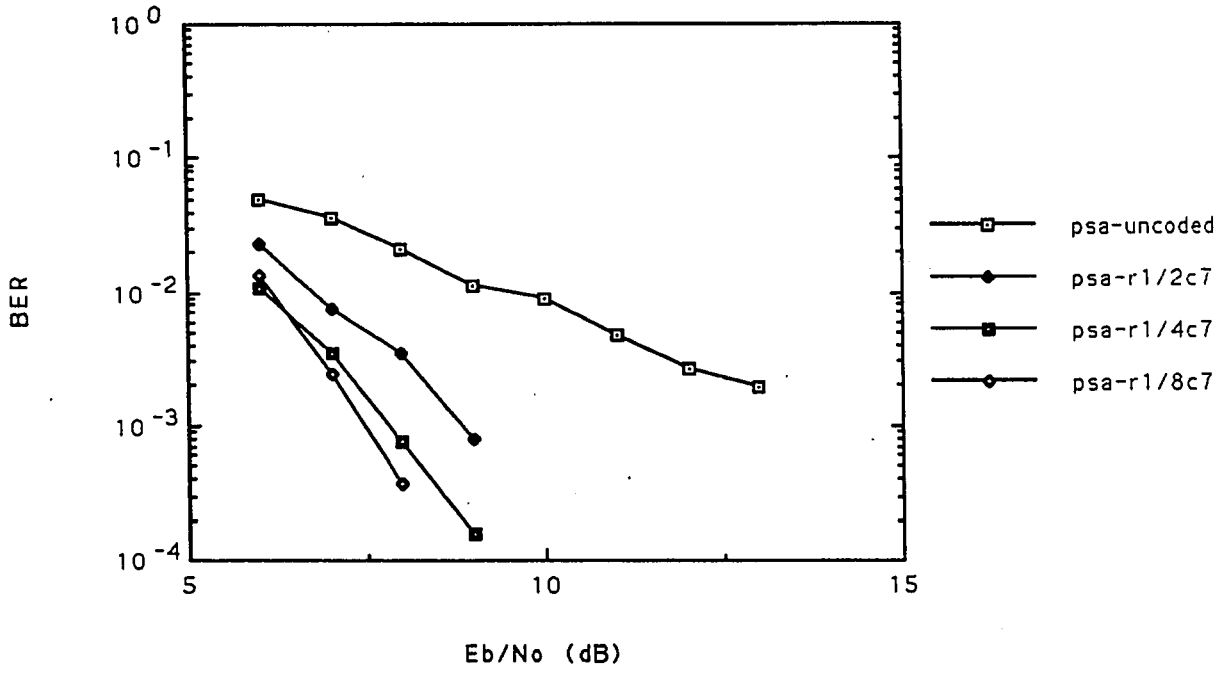

Figure 5.19: 5 path channel - 5 tap pilot symbol-aided RAKE receiver.

spectrum receiver would require a received E_b/N_o of 24dB (with rate 1/8 coding) for this channel. A gain of 12.8dB is obtained with the use of a RAKE receiver.

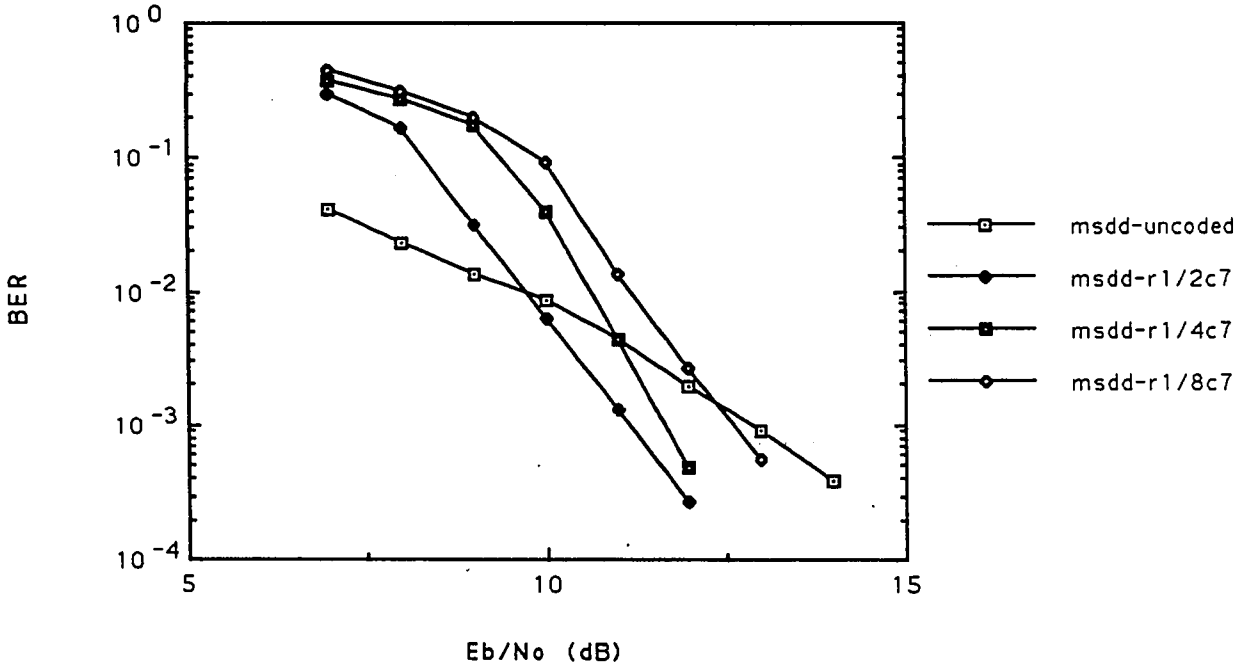

Figure 5.20: 5 path channel - 5 tap MSDD RAKE receiver.

The comparison of the three detection schemes is seen in Figure 5.21. The performance of uncoded pilot symbol-aided detection is slightly better than differential detection or MSDD at low values of E_b/N_o. However at higher values of E_b/N_o, uncoded pilot symbol-aided detection no longer provides the best results. Uncoded MSDD outperforms the other two detection schemes at these higher values of E_b/N_o. Rate 1/8 coded pilot symbol-aided coherent detection provides a 2.8dB gain over rate 1/2 coded differential detection. Rate 1/2 convolutional coded

MSDD performs about 1.7dB worse than that of coded differential detection.

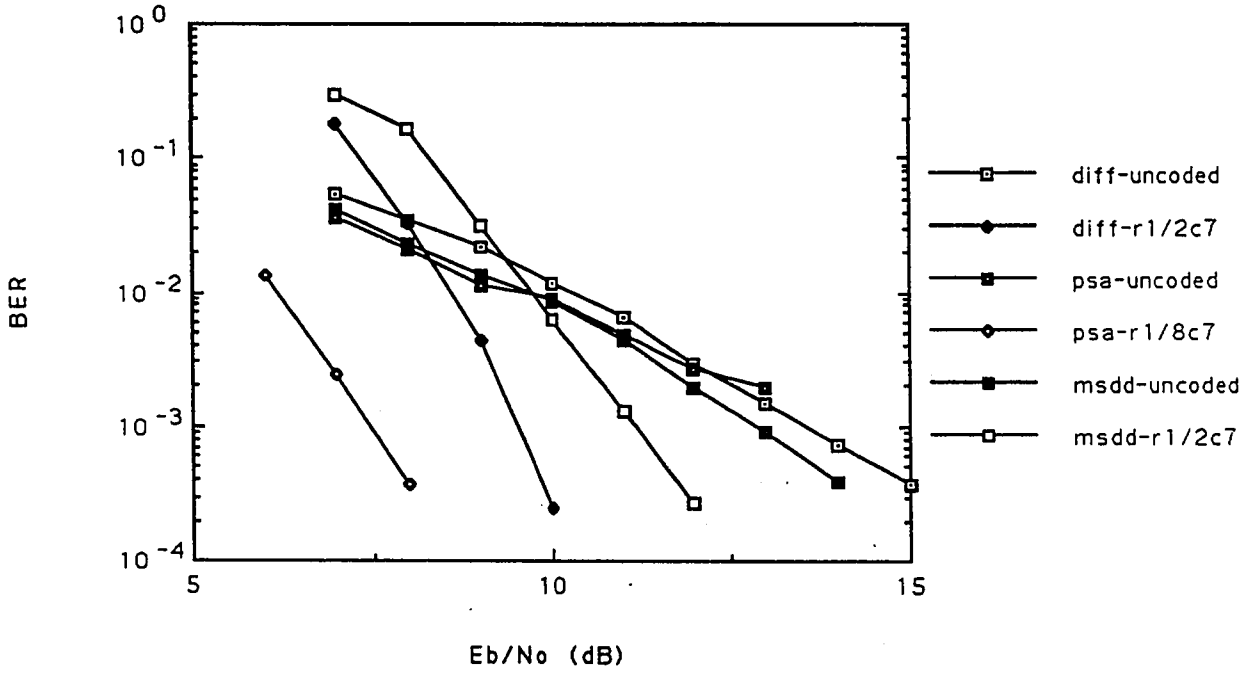

Figure 5.21: Comparison of different detection strategies for 5 path channel - 5 tap RAKE receiver.

5.3.6 5 Path Channel - Unequal Powers, 5 Tap RAKE

In Figures 5.22 to 5.25, a channel of 5 unequal paths is considered. In this case, all successive paths contain 2dB less energy than the previous path. These paths are received by a 5 tap RAKE.

Differential detection is shown in Figure 5.22. In this case, the best coding scheme is the rate 1/2 constraint length 7 convolutional code. The target bit error rate of 10^{-3} is obtained when E_b/N_o is about 10.1dB. From Figure 5.6, a single tap receiver would require that the received path have an $E_b/(N_o + I)$ of 10.5dB when rate 1/8 convolutional code is used. If we assume that the strongest path is received, we find that the receiver makes use of only 41% of the overall received E_b/N_o. Using the same calculation methods seen in the previous discussions, the required E_b/N_o for the conventional spread spectrum receiver is found to be 15dB. A gain of 4.5dB is obtained from using a 5 tap RAKE receiver for this channel condition.

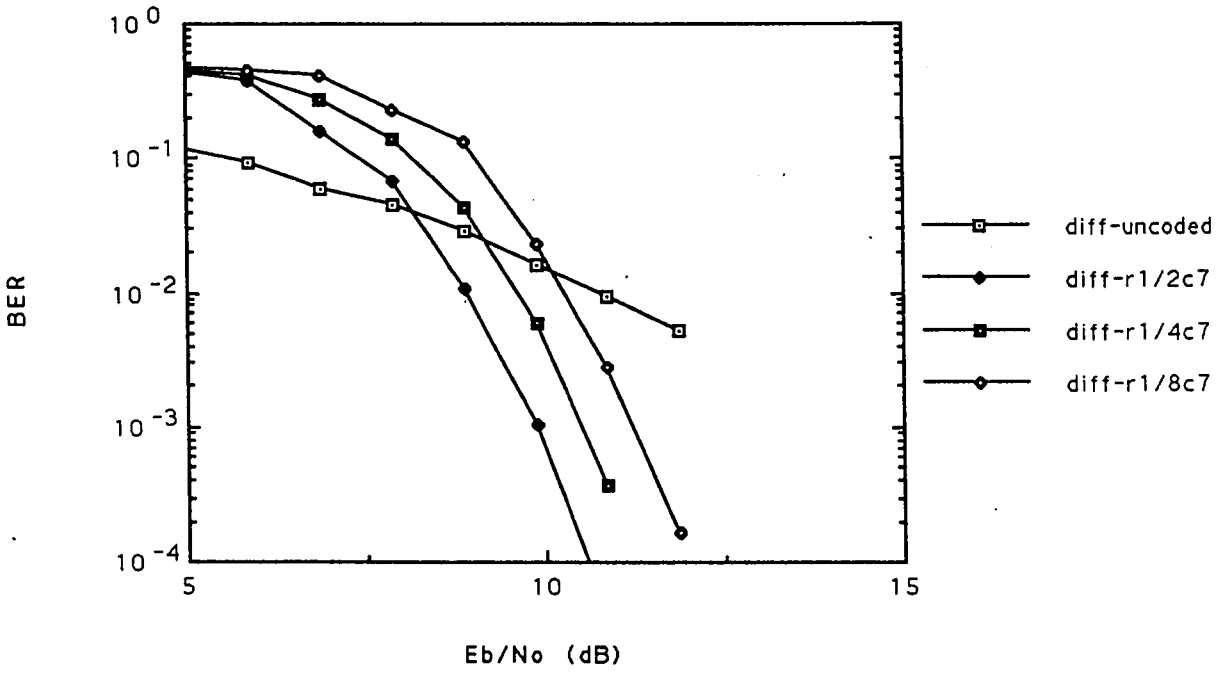

Figure 5.22: 5 paths of unequal power - 5 tap differential RAKE receiver.

Figure 5.23 demonstrates the use of pilot symbol-aided detection under these channel and receiver conditions. Rate 1/8 convolutional code is the best coding scheme in this case. The bit error rate of 10^{-3} occurs when E_b/N_o is about 7.7dB. A single tap receiver employing rate 1/8 convolutional code would require that E_b/N_o be 13.5dB. A gain of about 5.8dB is obtained when RAKE reception is used in this case.

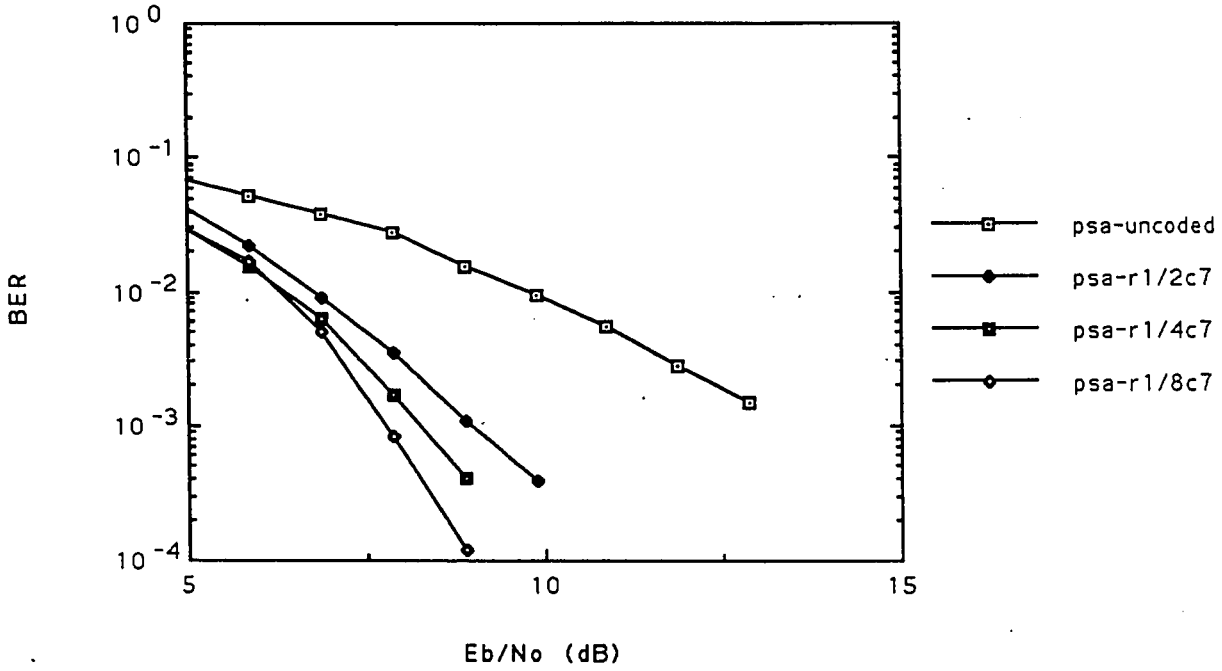

Figure 5.23: 5 paths of unequal power - 5 tap pilot symbol-aided RAKE receiver.

Figure 5.24 depicts the use of MSDD under these conditions. The target bit error rate is obtained when E_b/N_o is about 11.6dB. A single tap receiver with rate 1/8 convolutional code would require that E_b/N_o be about 17.7dB (provided the

strongest path is received by the single tap receiver). A gain of about 6.1dB is obtained when RAKE reception is used.

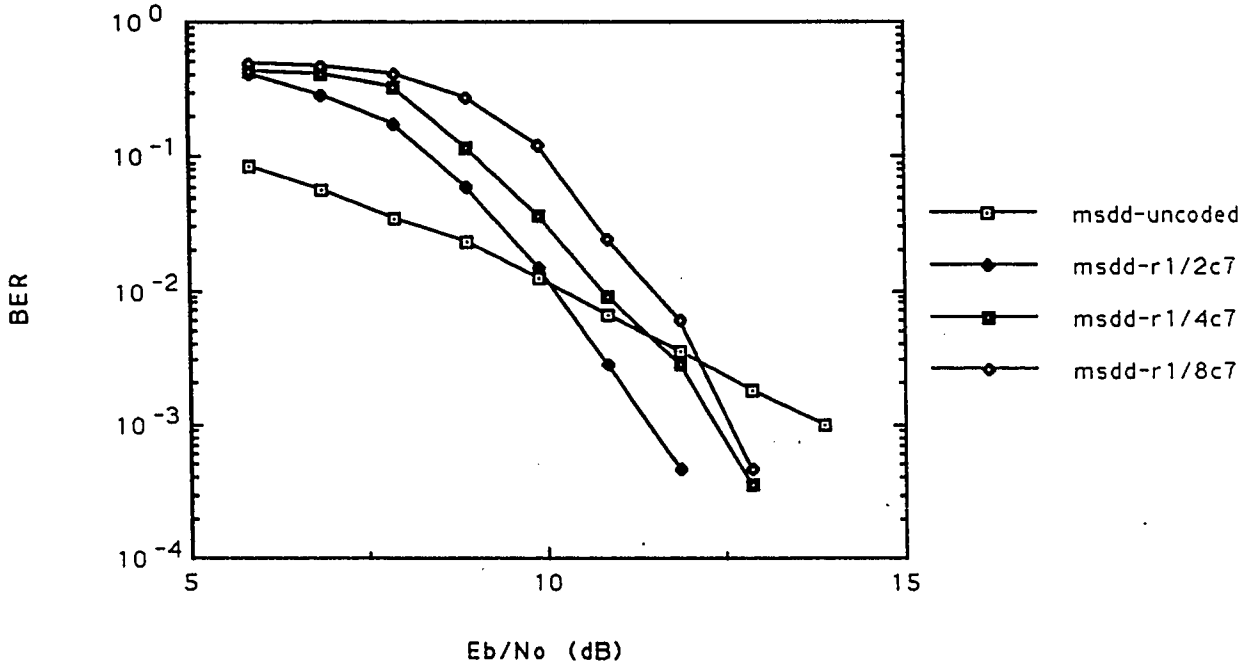

Figure 5.24: 5 paths of unequal power - 5 tap MSDD RAKE receiver.

The comparison of the different detection types for this system condition is shown in Figure 5.25. Uncoded pilot symbol-aided coherent detection outperforms the two other uncoded detection types. Uncoded MSDD slightly outperforms uncoded differential detection as well. Rate 1/8 convolutionally coded pilot symbol-aided detection provides a 2.5dB gain over rate 1/2 convolutionally coded differential detection. Coded MSDD is 1.5dB behind differential detection due to losses from the use of hard decision decoding.

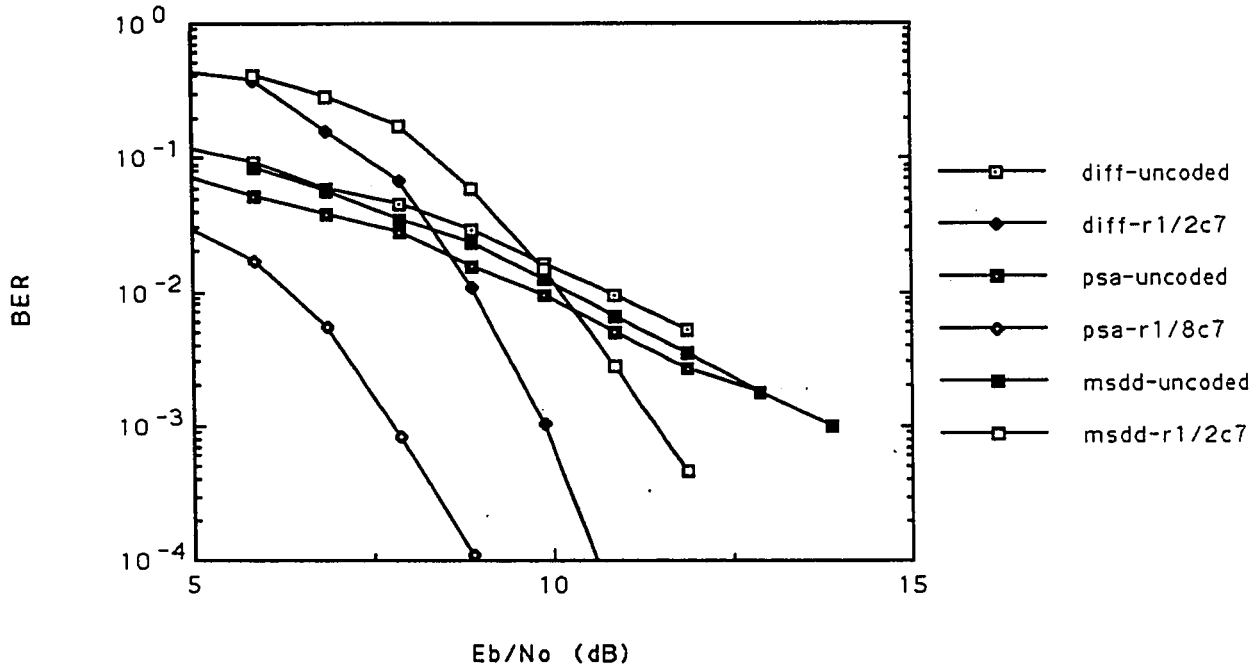

Figure 5.25: Comparison of different detection strategies for 5 paths of unequal power - 5 tap RAKE receiver.

Channel/Receiver	DD-r1/2	DD-r1/8	PSA-r1/2	PSA-r1/8	MSDD-r1/2	MSDD-r1/8
1 path 1 tap	11.1	10.5	11.7	**8.3**	14.7	12.8
1 path 5 taps	14.6	13.7	13.6	**10**	17.3	15.9
3 paths 1 tap	16.8	16.1	18	**13.9**	22.2	19.1
3 paths 5 taps	10.3	11.7	9.7	**8**	12.3	13.1
5 paths 1 tap	20.3	19	22	**16.3**	32.8	23.7
5 paths 5 taps	9.5	11.1	8.8	**7.5**	11.2	12.6
5 uneq. paths 1 tap	15.6	15	16.1	**13.5**	20.3	17.7
5 uneq. paths 5 taps	10.2	11.6	8.9	**7.7**	11.6	12.7

Table 5.2: Eb/No required for BER of 10^{-3} for a CDMA system with a processing gain of 128.

5.3.7 Summary

Table 5.2 shows the values of E_b/N_o required to obtain the target bit error rate for all detection schemes with rate 1/2 and 1/8 convolutional codes. For each channel condition, the best results are highlighted.

In the case when frequency-selective Rayleigh fading channels are received by single tap receivers, the results can be obtained by observing the single path single tap cases. Knowing how much energy is required for the target bit error rate for the single path, an estimate of the received signal energy of a frequency selective signal can be made.

The reception of frequency-selective signals with a RAKE receiver is shown to provide large gains over the use of a single tap receiver. These gains can be translated into larger capacities in a CDMA system.

If we assume that each user transmits a signal such that the receiver obtains a single user E_b/N_o of 20dB, equation (2.13) can be used to determine the maximum number of simultaneous users. This is shown in Table 5.3.

It can be seen from Table 5.2 that with the exception of frequency-nonselective channels, the use of RAKE reception greatly increases capacity. The values given in Table 5.2 are based on the assumption of perfect power control.

Channel/Receiver	DD-r1/2	DD-r1/8	PSA-r1/2	PSA-r1/8	MSDD-r1/2	MSDD-r1/8
1 path 1 tap	9	11	8	18	4	6
1 path 5 taps	4	5	5	12	2	3
3 paths 1 tap	2	2	1	4	0	1
3 paths 5 taps	10	8	13	20	7	5
5 paths 1 tap	0	1	0	2	0	0
5 paths 5 taps	14	9	16	22	9	6
5 uneq. paths 1 tap	3	3	2	5	0	1
5 uneq. paths 5 taps	11	8	16	21	8	6

Table 5.3: Maximum number of simultaneous users for a CDMA system with a processing gain of 128 for a single user E_b/N_o of 20dB.

Chapter 6

Conclusions

The use of RAKE reception in land mobile communications has been considered for some time. The receiver has one tap for each chip in the PN sequence, and thus the RAKE receiver in this study would employ 128 taps. If the bit rate is 10 kbps, a chip time would be about 0.8 microseconds. The typical delay spread of a land mobile channel is about 5 microseconds. All received information from the channel would therefore be received on 1 to 10 adjacent taps. An algorithm could be implemented which determines which group of taps contains the highest average energy. The receiver may then choose the 5 most likely taps to contribute to the final decision.

From the performance curves given in Section 5.3, the following conclusions can be drawn:

(i) Diversity reception of frequency-selective Rayleigh faded signals with RAKE receivers provides large gains over the reception of a single path. These gains can then be translated into larger capacities in CDMA systems.

(ii) Lower rate codes perform better than higher rate codes when coherent detection is used in both AWGN and Rayleigh fading channels. This is generally not true when differential detection is used.

(iii) In all cases, rate 1/8 convolutionally encoded pilot symbol-aided coherent detection provides the target bit error rate at the lowest signal energy, and thus provides the largest channel capacity for the conditions described in this thesis.

(iv) Pilot symbol-aided coherent detection can suppress the effects of noisy taps much better than differential detection and thus this technique requires a less complex noisy tap elimination algorithm.

(v) Uncoded MSDD, with a detection window of 3 symbols, performs better than uncoded differential detection in all cases.

(vi) In the frequency-selective cases, rate 1/2 constraint length 7 convolutional code is the best coding scheme for the two different differential detection schemes, while rate 1/8 constraint length 7 code is best in all cases for pilot symbol-aided coherent detection.

In all frequency-selective cases where RAKE reception is used, pilot symbol-aided coherent detection with rate 1/8 constraint length 7 convolutional code provided the best performance. Therefore, in a land mobile communications channel, which is subjected to frequency-selective Rayleigh fading, the choice of pilot symbol-aided detection with rate 1/8 constraint length 7 convolutional code appears to be a good receiver implementation under the conditions presented in this thesis.

6.1 Recommendations for Further Study

The performance of uncoded MSDD compared to that of uncoded differential detection demonstrated that MSDD is quite adaptable to a RAKE receiver environment. However, the implementation of the MSDD receiver required that a decision be made by the detector, making soft decision decoding impossible. By modifying the receiver in order to allow soft decision decoding, the performance of the MSDD RAKE receiver might improve. Larger detection windows could also be considered. However, this method results in an increase in receiver complexity.

Low rate codes performed well for coherent detection in all cases discussed. Lower rate codes such as rate 1/16 or low rate concatenated coding schemes may improve

performance even more. However, one must take into account the interleaving delay and complexity when employing lower rate codes.

The results show that the higher rate codes perform better when multiple paths are received and combined with both types of differential detection. Perhaps even higher rate codes such as rate 2/3 would provide more gain at a bit error rate of 10^{-3} for these detection schemes.

The effect of path delays when the delay is not a multiple of the chip time should also be investigated. When a fraction of the path's energy is received on adjacent taps, loss will occur when the path is recombined. It should be determined which detection scheme recombines the divided path with the least loss. Since it was noted that pilot symbol-aided coherent detection best suppressed noisy taps, it would seem likely that this detection scheme would recombine the divided paths with the least loss.

Bibliography

[1] R.J. Lynch, "PCN: Son of Cellular? The Challenges of Providing PCN Service", *IEEE Comm. Mag.*, vol. 44, no. 2, pp. 56-57, Feb. 1991.

[2] D.G. Smith, "Spread Spectrum for Wireless Phone Systems: The Subtle Interplay Between Technology and Regulation", *IEEE Comm. Mag.*, pp. 44-46, vol. 44, no. 2, Feb. 1991.

[3] D.L. Schilling L.B. Millstein, R.L. Pickholtz, W.Biederman, M. Kullbeck, "Future Personal Communications and Spread Spectrum Management", *Spread Spectrum Workshop*, Montebello, May 1991.

[4] K.S. Gilhousen, I.M. Jacobs, R. Padovani, A.J. Viterbi, L.A. Weaver, Jr., C.E. Weatley III, "On the Capacity of a Cellular CDMA System", *IEEE Trans. Veh. Technol.*, vol. 40, pp 303-312, May 1991.

[5] A. Yongaçoglu, R.G. Lyons, B.A. Mazur, "Comparison of FDMA and CDMA for Second Generation Land-Mobile Satellite Communications", *Proceedings of the Second International Mobile Satellite Conference*, Ottawa, June 1990.

[6] W.C.Y. Lee, "Overview of Cellular CDMA", *IEEE Trans. Veh. Tech.*, vol. 40, no. 2, pp. 291-301, May 1991.

[7] M.J. Marcus, "Regulatory Policy for Civil Use of Spread Spectrum in the USA", *Spread Spectrum Workshop*, Montebello, May 1991.

[8] A.J. Viterbi, "When Not to Spread Spectrum - A Sequel", *IEEE Commun. Mag.*, vol. 23, no. 4, pp. 12-17, April 1985.

[9] E. Geranoitis, B. Ghaffari, "Performance of Binary and Quaternary DS SSMA Systems With Random Signature Sequences", *IEEE Trans. Comm.*, vol. 39, no. 5, pp. 713-724, May 1991.

[10] J.G. Proakis, *Digital Communications*, 2nd Ed., New York: MacGraw-Hill, 1989.

[11] J. D. Parsons, D.A. Demery, A.M.D. Turkmani, "Sounding Techniques for Wideband Mobile Radio Channels: A Review", *IEE Proceedings-I*, vol. 138, no. 5, pp. 437-446, Oct. 1991.

[12] D. Divsalar and M.K. Simon, "Multiple-Symbol Differential Detection of MPSK", *IEEE Trans. Comm.*, vcol. COM-38, pp. 300-308, March 1990.

[13] D. Makrakis, A. Yongaçoğlu, K.Feher,"Novel Receiver Structures for Systems Using Differential Detection", *IEEE Trans. Veh. Tech.*, vol VT-36, pp. 71-77, May 1987.

[14] G.L. Turin, et al.,"A Statistical Model of Urban Multipath Propagation", *IEEE Trans. Veh. Tech.*, vol. 21, pp 1-9, Feb. 1972.

[15] R.C. Dixon, "Why Spread Spectrum", *IEEE Comm. Mag.*, vol. 13, no. 7, July 1975.

[16] D.J. Torrieri, *Principles of Secure Communication Systems*, Dedham, MA.: Artech House, 1985.

[17] R.C. Dixon, *Spread Spectrum Systems*, 2nd Ed., New York: Wiley, 1984.

[18] R.E. Ziemer and R.L. Peterson, *Digital Communications and Spread Spectrum Systems*, New York: MacMillan, 1985.

[19] S.S. Rappaport, D.M. Greico,"Spread-Spectrum Signal Acquisition: Methods and Technology", *IEEE Comm. Mag.*, vol. 22, no. 6, June 1985.

[20] A.J. Viterbi,"Spread Spectrum Communications - Myths and Realities", *IEEE Comm. Mag.*, vol. 17, no. 5, pp. 11-18, May 1979.

[21] T.T. Ha, *Digital Satellite Communications*, 2nd Ed., New York: MacGraw-Hill, 1990.

[22] M.K. Simon, J.K. Omura, R.A. Scholtz, B.K. Levitt, *Spread Spectrum Communications*, vol.1, Rockville, Md.: Computer Science Press, 1985.

[23] A.J. Viterbi, "Modulation and Coding Performance of the Power-Controlled

Direct-Sequence CDMA Cellular Channel", *Spread Spectrum Workshop*, Montebello, May 1991.

[24] G.L. Turin, "Introduction to Spread-Spectrum Antimultipath Techniques and Their Application to Urban Digital Radio", *Proc. IEEE*, vol. 68, pp 328-353, March 1980.

[25] G.L. Turin, "The Effects of Multipath and Fading on the Performance of Direct-Sequence CDMA Systems", *IEEE Trans. Veh. Tech.*, vol VT-33, no. 3, pp. 213-219, Aug. 1984.

[26] M. Kavehrad, B. Ramamurthi, "Direct-Sequence Spread Spectrum with DBPSK Modulation and Diversity for Indoor Wireless Communications", *IEEE Trans. Comm.*, vol. COM-35, no. 2, pp. 224-236, Feb. 1987.

[27] M. Kavehrad, P.J. McLane, "Performance of Low-Complexity Channel Coding and Diversity for Spread Spectrum in Indoor, Wireless Communications", *AT&T Tech. J.*, vol. 64, no, 10, pp. 1927-1965, Oct. 1985.

[28] H. Oschner, "Direct-Sequence Spread-Spectrum Receiver for Communication on Frequency-Selective Fading Channels", *IEEE J. Sel. Areas Comm.*, vol. SAC-5, no.2, pp. 188-193, Feb. 1987.

[29] W.H. Lam, R. Steele, "Performance of Direct-Sequence Spread-Spectrum Multiple-Access Systems in Mobile Radio", *IEE Proceedings-I*, vol. 138, no. 1, pp. 1-14, Feb. 1991.

[30] F. Davarian, "Mobile Digital Communications via Tone Calibration", *IEEE Trans. Veh. Tech.*, vol. VT-36, no. 2, pp 55-62, May 1987.

[31] M.L. Moher and J.H. Lodge, "TCMP - a modulation and coding strategy for Rician channels", *J. Sel. Areas Comm.*, vol SAC-7, no.12, pp. 1347-1355, Dec. 1989.

[32] R.E. Blahut, *Digital Transmission of Information*, Chapter 11, Reading: Addison-Wesley, 1990.

[33] D.G. Brennan, "Linear Diversity Combining Techniques", *Proc. IRE.*, vol.

47, pp. 1075-1102, June 1959.

[34] R. Price and P.E. Green, "A Communication Technique for Multipath Channels", *Proc. IRE.*, vol. 46, pp. 555-570, March 1958.

[35] J.K. Cavers, "An Analysis of Pilot Symbol Assisted Modulation for Rayleigh Fading Channels", *IEEE Veh. Tech.*, vol. 40, no. 4, pp. 686-693, Nov. 1991.

[36] S. Lin, D.J. Costello, Jr., *Error Control Coding: Fundamentals and Applications*, Englewood Cliffs, N.J.: Prentice-Hall, 1983.